ELSEVIER

Physica D 100 (1997) 1–40

PHYSICA D

Review

The limited effectiveness of normal forms: A critical review and extension of local bifurcation studies of the Brusselator PDE

Ralf W. Wittenberg *, Philip Holmes

Program in Applied and Computational Mathematics, Fine Hall, Washington Road, Princeton, NJ 08544, USA

Received 2 May 1996; accepted 3 June 1996
Communicated by C.K.R.T. Jones

Abstract

The detection and unfolding of degenerate local bifurcations provides one of very few generally applicable analytical tools for studying complex dynamics in systems of arbitrarily high dimension. Using the Brusselator partial differential equations (PDEs) (Prigogine and Lefever, 1968) as motivation and main example, we critically review this method. We extend and correct previous calculations, presenting explicit formulae from which normal forms accurate to third order may be computed, and for the first time we carefully compare bifurcations and dynamics of these normal forms with those of the untransformed systems restricted to a center manifold, and with Galerkin and finite difference approximations of the original PDE. While judicious use of symbolic manipulations makes feasible such high-order center manifold and normal form calculations, we show that the conclusions drawn from them are of limited use in understanding spatio-temporal complexity and chaos. As Guckenheimer (1981) argued, the method permits proof of existence of quasi-periodic motions and, under mild genericity assumptions, Šil'nikov chaos (sub-shifts of finite type), but the parameter and phase space ranges in which these results may be applied are extremely small.

1. Introduction

Over the last 20–25 years, the theory of low-dimensional dynamical systems has been extensively developed to yield insights on complex behavior, including "chaos", that may occur in deterministic systems with few degrees of freedom. However, many models of physical interest that exhibit spatio-temporal patterning and chaos have (at least in principle) infinitely many degrees of freedom, and it is an important question to what extent essentially low-dimensional methods can be rigorously extended to such systems, particularly those described by partial differential equations (PDEs).

One approach, implicit in the work of Thom (1975) and laid out in texts such as Guckenheimer and Holmes (1986); Golubitsky et al. (1988), goes as follows: Using conventional linear stability methods, one locates an "interesting" degenerate bifurcation (of codimension ≥ 2) of a known solution in a PDE, restricts to a center

* Corresponding author.

PII S0167-2789(96)00187-X

manifold, computes the normal form and unfolds the resulting low-dimensional vector field. The procedure can even be partially automated via computer algebra packages such as MATLAB, Maple or Mathematica (Rand and Armbruster, 1987). Using this method, around 1980 John Guckenheimer (1981) produced an early example of an autonomous PDE with chaotic behavior. He did this by showing that Brusselator reaction–diffusion equation (Prigogine and Lefever, 1968) exhibits a codimension two bifurcation occurring on a three-dimensional center manifold which, when "generically" unfolded, exhibits Šil'nikov homoclinic cycles and hence chaos (Šil'nikov, 1965, 1970).

In this paper we return to the Brusselator problem and make explicit computations at higher order than Guckenheimer's. In the process, we develop general expressions for the coefficients of the normal form associated with a simple zero and a pure imaginary pair of eigenvalues (the transcritical/Hopf bifurcation), and, in doing so, extend and correct erroneous formulae which have appeared in the literature. However, our main goal is to investigate the usefulness of normal form transformations in reaction–diffusion problems more generally, and to show that the ranges in which they are effective can be *extremely* small, so that the corresponding "chaotic" solutions will be essentially undetectable in practice. In particular, Guckenheimer's choice of mode/parameter values gives a range of parameter/state variables of the order of 10^{-5}, although we show that other parameter ranges exist in which this increases to 10^{-3}.

The paper is organised as follows. After introducing the Brusselator and the general unfolding approach in Section 2, we describe the specific codimension two bifurcation of interest in Section 3 and review some relevant details of normal form transformations in Section 4, not all of which appear to be widely known. Thus prepared, in Section 5 we return to the Brusselator problem. We compare analytical and numerical bifurcation results on the normal form and in the original PDE, locating and illustrating periodic and quasi-periodic motions of small but finite amplitude. In doing so we investigate in some detail the derivation of higher-order normal form transformations, including unfolding parameters, which are necessary to determine the stability types of secondary bifurcations to invariant tori (Langford, 1979; Scheurle and Marsden, 1984) and to characterize potentially chaotic solutions emerging from Šil'nikov-type homoclinic orbits. Explicit computational details are relegated to the appendices.

This paper may be read as an instructional case study of how center manifold and normal form techniques can be applied to PDEs, as well as a cautionary tale concerning the limitations of low-dimensional dynamics. We assume that the reader is familiar with simple (codimension one) bifurcations including the Hopf and transcritical, and with the elements of applied dynamical systems theory which may be found in texts such as Guckenheimer and Holmes (1986) and Arrowsmith and Place (1990).

2. A low-dimensional approach to "complex systems"

2.1. Brusselator reaction–diffusion system

Our central example will be the model trimolecular chemical reaction system known as the "Brusselator", which was originally proposed (Prigogine and Lefever, 1968; Nicolis and Prigogine, 1977) as a model for "dissipative structure" or "self-organization", since it is capable of sustaining oscillations and heterogeneous spatial structure in the presence of diffusion. Extensive linear and bifurcation analyses have been performed on this system, see, e.g., Auchmuty and Nicolis (1975, 1976) and Keener (1976). Here we only briefly outline relevant results.

2.1.1. Reaction kinetics and equations

The model reaction kinetics are given by

$$A \xrightarrow{k_1} X, \qquad 2X + Y \xrightarrow{k_2} 3X, \qquad B + X \xrightarrow{k_3} Y + C, \qquad X \xrightarrow{k_4} D,$$

leading to the overall reaction

$$A + B \to C + D;$$

but we consider the dynamics only of the intermediates X and Y.

We take the reaction equations in a one-dimensional domain, and nondimensionalize, to obtain a system of reaction–diffusion equations for X and Y. We perturb these equations about the homogeneous steady state, $X = A + u$, $Y = B/A + v$, to give

$$\frac{\partial u}{\partial t} = D_1 \frac{\partial^2 u}{\partial \xi^2} + (B-1)u + A^2 v + h(u,v), \qquad \frac{\partial v}{\partial t} = D_2 \frac{\partial^2 v}{\partial \xi^2} - Bu - A^2 v - h(u,v), \tag{1}$$

where

$$h(u,v) \equiv u^2 v + 2Auv + \frac{B}{A}u^2.$$

Initial conditions are typically small perturbations from the equilibrium $u = v = 0$. Following Guckenheimer (1981), we impose Dirichlet boundary conditions

$$u(0,\cdot) = u(\pi,\cdot) = 0, \qquad v(0,\cdot) = v(\pi,\cdot) = 0,$$

corresponding to fixing the concentrations A and B at the boundaries of the domain.

2.1.2. Codimension one bifurcation in the Brusselator

In the absence of diffusion, the planar ODE system undergoes a *Hopf* bifurcation at $B = 1 + A^2$, where the eigenvalues are $\pm i\omega$; this corresponds to the onset of homogeneous oscillations. This property led to much of the initial interest in the Brusselator as a prototypical chemical oscillator (Prigogine and Lefever, 1968), and paved the way for the study of more realistic chemical models such as those of the Belousov–Zhabotinskii reaction (e.g., Field et al. (1972) and Field and Noyes (1974)).

In the presence of diffusion, we represent the solutions to (1) as Fourier sine series (satisfying the Dirichlet boundary conditions), $u(\xi,t) = \sum_{l=1}^{\infty} \beta_l(t) \sin l\xi$, $v(\xi,t) = \sum_{l=1}^{\infty} \gamma_l(t) \sin l\xi$. We note $\beta_l = 0, \gamma_l = 0$ is always a solution, and that the linearized stability of this trivial solution to the lth Fourier mode is obtained from the eigenvalues of the matrix

$$E_l \equiv \begin{pmatrix} B - 1 - l^2 D_1 & A^2 \\ -B & -A^2 - l^2 D_2 \end{pmatrix}. \tag{2}$$

It is possible to vary a parameter, such as B, so that the zero solution for one of the modal amplitudes, say β_k, becomes unstable in a *transcritical* bifurcation, while all others remain stable. In the PDE this corresponds to the spontaneous formation of a stable, spatially inhomogeneous state in mode k, in a *Turing* bifurcation (Turing, 1952) (see Fig. 1 for such a solution for $k = 3$). Such "spontaneous" pattern formation has been studied extensively, and numerous applications proposed in chemical and ecological systems, as well as in developmental biology (Levin and Segel, 1985; Murray, 1989; Harrison, 1993).

The Hopf and transcritical codimension one bifurcations discussed above are straightforwardly detected in the PDE, and the low-dimensional theory carries over directly and unambiguously. (The latter bifurcation may be replaced by a saddle–node or pitchfork bifurcation, depending, respectively, on whether a trivial solution always exists, and on the presence of symmetry.) However, a standard picture for the generation of complex spatial structure

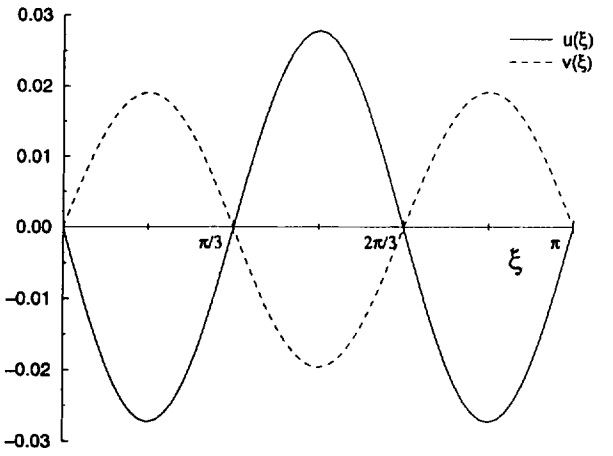

Fig. 1. Inhomogeneous steady state with $k = 3$ for the Brusselator, $B = 3.1035$, $A^2 = 1.7035$, $D_1 = 0.10$, $D_2 = 0.30$; i.e. $\varepsilon = -5 \times 10^{-6}$, $\delta = 0.004$.

is one of successive bifurcations from the initial spatially inhomogeneous state; and the analytical "proof" of such a scenario rapidly becomes intractable, even for a model problem such as (1). Thus, one supposes that a second parameter (e.g. A) can be varied independently to make the two codimension one bifurcations coincide in a degenerate singularity that can be *unfolded* to reveal all possible neighboring behaviors at once.

2.2. *An approach to spatio-temporal complexity: Codimension two bifurcation*

The codimension two bifurcation arising from the coincidence of the above-mentioned codimension one bifurcations, that is the saddle–node/Hopf or transcritical/Hopf bifurcation, has been studied extensively (Guckenheimer and Holmes, 1986; Arnol'd, 1988; Chow et al., 1994), and, together with other bifurcations of codimension higher than one, displays a surprising richness of behavior (the double zero eigenvalue bifurcation was studied in Schaeffer and Golubitsky (1981)). The analysis proceeds via the normal form, as discussed below; and the properties of the system depend on the coefficients in the normal form. In some cases, one essentially has just a superposition of the contributing codimension one bifurcations, while in others, more complex, interactive behavior may occur, including the presence of a secondary Hopf bifurcation leading to formation of a torus (two-frequency motion, in general quasi-periodic), and a Šil'nikov homoclinic connection, implying chaos. This will be described below, but we note here that the complicated temporal dynamics in modal amplitudes occurring in the vicinity of this bifurcation correspond to complex spatio-temporal behavior in the original PDE involving dynamical interactions of two Fourier modes (for more information, see the above references and the original papers referred to therein).

2.2.1. *Guckenheimer's observation: Chaos in the Brusselator*

Motivated by numerical evidence for complexity in the Brusselator (Kuramoto, 1978), Guckenheimer (1981) observed that there were choices of parameter values for A, B, D_1 and D_2 for which this codimension two bifurcation occurs; specifically, for which the linearized system has one zero and a pair of pure imaginary eigenvalues, and there is interaction between a Hopf bifurcation in mode 1 and a transcritical bifurcation in mode k. In addition, the parameter values and wave number k may be chosen so that the quadratic normal form coefficients for the Brusselator have the appropriate signs for the richest behavior possible in the transcritical/Hopf bifurcation, including torus creation and chaos, to occur.

Guckenheimer's result generated a great deal of interest, as this was one of the first cases in which (spatio-temporal) chaos, albeit of a simple kind, had been demonstrated to exist in a PDE (in 1979, Holmes and Marsden had provided the first example of a periodically perturbed chaotic PDE, see, Holmes and Marsden (1981)). This bifurcation has subsequently been studied in more depth, frequently with specific reference to the Brusselator (Guckenheimer, 1984, 1986; Scheurle and Marsden, 1984; Armbruster et al., 1985) and to the parameter values Guckenheimer proposed; indeed, a large variety of complex behavior predicted in the vicinity of this bifurcation has been claimed to occur in the Brusselator, with implications for other pattern-forming systems (Armbruster et al., 1985).

In his work, Guckenheimer implicitly proposed a program for detecting a torus (two-frequency spatio-temporal dynamics) and chaos in a PDE:

(1) Perform a Galerkin approximation (and suitable change of variables) to obtain an (infinite) system of ODEs for the time-dependent modal coefficients.
(2) Choose parameter values for which the desired bifurcation takes place.
(3) Restrict the equations onto the critical modes, introducing nonlinear (center manifold) corrections to the requisite order.
(4) Calculate normal form coefficients, and use the "simple" normal form to predict for which values of unfolding parameters "interesting" behavior such as the torus and chaos occurs.
(5) Relate the normal form results back to the original system, by relating unfolding parameters to the PDE parameters, and hence detect the parameter region in which invariant tori and chaos occur in the PDE.

This program represents one of the very few explicit and rigorous tools for bifurcation analysis in nonlinear PDEs. It is therefore important to assess its feasibility and effectiveness.

2.2.2. *Center manifold and normal form techniques*

Reduction to the center manifold is now a standard technique (Carr, 1981; Guckenheimer and Holmes, 1986); briefly, the center manifold is a graph $y = h(x)$ for the stable modes y over the space spanned by the center modes x, tangent to the center eigenspace at the origin, so that the lowest-order terms are quadratic, $h = \mathrm{O}(2)$. For the system

$$\dot{x} = Ax + f(x, y), \qquad \dot{y} = By + g(x, y), \tag{3}$$

where the eigenvalues of A have zero and those of B have negative real parts, the equation determining the center manifold is

$$Dh(x)(Ax + f(x, h(x))) = Bh(x) + g(x, h(x)), \tag{4}$$

and, if (4) can be solved (approximately) for $h(x)$, the reduced system may be written by substitution of $y = h(x)$

$$\dot{x} = Ax + f(x, h(x)). \tag{5}$$

Strictly, (5) is a projection of the full vector field, restricted to the (approximate) center manifold, onto the center eigenspace, but it is normally referred to as a center manifold reduction. In practice, one computes h to a finite order of accuracy, so that (5) is approximated by a truncated Taylor series.

The method of normal forms (Takens, 1974; Guckenheimer and Holmes, 1986; Arnol'd, 1988; Chow et al., 1994) enables us to analyze the behavior of a vector field near a singularity by reducing it via a suitable change of

coordinates, valid in a neighborhood of the origin, to a simpler form more amenable to analysis. Normal forms are computed from (5) by near-identity coordinate changes, of the form

$$x = z + k(z), \quad k(z) = \sum_{j \geq 2} k_j(z), \quad k_j(z) = \mathrm{O}(|z|^j),$$

under which (5) assumes the form

$$\dot{z} = (I + Dk(z))^{-1}[Az + Ak(z) + f(z + k(z), h(z + k(z)))]. \tag{6}$$

Expanding (6) order by order, one then chooses the components of k successively to eliminate as many terms as possible in the final equation. In particular, the matrix A determines *resonant* terms, and the standard theory (Guckenheimer and Holmes, 1986; Arnol'd, 1988) indicates that nonresonant terms may always be eliminated from the normal form. Details for the transcritical/Hopf bifurcation are given in Appendix A. We note that Elphick et al. (1987) have shown how the reduction and normal form calculations can be combined in a single step; however, we find the method sketched above to be more transparent.

2.2.3. Motivation for and outcome of our studies

The original motivation for the investigations reported here was to carry out the above program and hence confirm the presence of chaos in the Brusselator directly. In attempting this, we learned more than we had anticipated about the validity and predictive power of normal form transformations in such "large" systems. We discovered not only inherent complications and difficulties in carrying out this investigation, but also that the results were not as useful as we had hoped. Specifically, whereas the bifurcation and its attendant complexities are indeed present, they appear to have a negligible effect on the dynamics, in the sense of being relevant in a vanishingly small parameter régime, and leading to solutions that are very small perturbations of the homogeneous solution. The normal form, furthermore, is quantitatively a poor predictor of bifurcation points in the full system, except very near the codimension two bifurcation point itself.

The above conclusions will be motivated and discussed in greater depth in what follows, after we have set up the problem and described the calculations in some detail; but in summary, it appears that (at least for this particular case) the low-dimensional paradigm for studying complex systems, while rigorously establishing the existence of a torus and chaos, applies in such a small parameter régime as to be practically irrelevant in understanding the complex dynamics that originally motivated it.

3. Transcritical/Hopf bifurcation

To motivate our analysis of the transcritical/Hopf bifurcation in the Brusselator, and the calculation of the relevant normal form coefficients, we briefly review pertinent results demonstrating complex behavior in this bifurcation. For more details, see Guckenheimer (1981), Guckenheimer and Holmes (1986), Gaspard (1993) and Chow et al. (1994). We begin by considering a three-dimensional ODE system in which, for certain suitable parameter values, the Jacobian matrix has a zero eigenvalue and a pair of pure imaginary eigenvalues; that is, a linear transformation exists which converts the system at the bifurcation point into the form

$$\dot{x} = -\omega y + f(x, y, z), \qquad \dot{y} = \omega x + g(x, y, z), \qquad \dot{z} = h(x, y, z), \tag{7}$$

where $\dot{(\,)} \equiv \mathrm{d}/\mathrm{d}t$. (The relevance to our example, via the reduction of the PDE to (7) using center manifold techniques, will be discussed in Section 5.2.) In this system, it is natural to change to cylindrical polar coordinates,

in view of the rotational SO(2) symmetry at linear order in the x–y plane. To predict the local properties of the vector field (7) near the bifurcation point, we appeal to the method of normal forms, outlined in Section 2.2.

3.1. Quadratic normal form and unfolding

We defer a more detailed discussion of the normal form analysis of (7) to Section 4 and Appendix A, and merely quote results here. It is fairly straightforward to confirm, by analysis of resonant terms (Guckenheimer and Holmes, 1986; Arnol'd, 1988), that a change of variables exists which transforms (7) to the normal form (to quadratic order)

$$\dot{r} = a_1 r z + \mathrm{O}(3), \tag{8}$$

$$\dot{z} = b_1 r^2 + b_2 z^2 + \mathrm{O}(3), \tag{9}$$

$$\dot{\theta} = \omega + c_1 z + \mathrm{O}(2), \tag{10}$$

where $\mathrm{O}(n)$ denotes terms of order n in r and z. Note that the resonant terms are precisely those that respect the SO(2) symmetry of the linear part of the original system (7), leading to the $r \to -r$ symmetry in the normal form. Also, as a consequence the $\dot{\theta}$ equation decouples from the other two (in fact at all orders), and may therefore be neglected in studies of the normal form, although it is important for deriving the implications for the full flow. We will ignore the $\dot{\theta}$ equation for now.

Guckenheimer (1981) has given the expressions for the normal form coefficients for this case, in terms of derivatives of the original nonlinear functions f, g and h of (7); only the quadratic terms in the Taylor expansion contribute, and these are fairly straightforward to obtain from a consideration of resonant terms:

$$a_1 = \tfrac{1}{2}(f_{xz} + g_{yz}), \tag{11}$$

$$b_1 = \tfrac{1}{4}(h_{xx} + h_{yy}), \tag{12}$$

$$b_2 = \tfrac{1}{2}h_{zz}, \tag{13}$$

$$c_1 = \tfrac{1}{2}(g_{xz} - f_{yz}). \tag{14}$$

The above formulae for a_1, b_1 and b_2 are not unique, these coefficients being dictated by a choice of scaling for r and z in (8) and (9). To facilitate comparison between different systems and reduce the number of parameters, it is convenient to rescale the normal form, fixing some coefficients; specifically, we choose the coefficient of $z^2\partial_z$ to be -1, and that of $r^2\partial_z$ to be ± 1. Assuming $b_1, b_2 \neq 0$, the rescaling $r \to \sqrt{|b_1 b_2|}r$, $z \to -b_2 z$, gives the planar system

$$\dot{r} = arz + \mathrm{O}(3), \tag{15}$$

$$\dot{z} = br^2 - z^2 + \mathrm{O}(3), \tag{16}$$

where $a = -a_1/b_2$, $b = \mathrm{sign}(-b_1 b_2) = \pm 1$, and we have omitted the $\dot{\theta}$ component. It is this normalized form that we use to develop the theory, and compare different systems with each other.

The normal form (15) and (16) and its unfolding have already been studied in some depth (Langford, 1979; Guckenheimer, 1981; Scheurle and Marsden, 1984; Guckenheimer and Holmes, 1986; Gaspard, 1993; Chow et al., 1994), and we refer the reader to these works for details; we follow in particular the approach of Guckenheimer and Holmes (1986) (note that the 1986 and subsequent printings correct errors in the treatment of this bifurcation in the first 1983 edition). As indicated there, in the "most general" case a universal unfolding of (15) and (16) is given by

$$\dot{r} = \varepsilon r + arz + \mathrm{O}(3), \tag{17}$$

$$\dot{z} = \delta + br^2 - z^2 + \mathrm{O}(3) \tag{18}$$

(the odd symmetry $r \to -r$ must be retained in the unfolding), and this is the unfolding that has usually been studied, corresponding to coupling a saddle–node and Hopf bifurcation.

For application to the Brusselator, we must consider rather the unfolding

$$\dot{r} = \varepsilon r + arz + \mathrm{O}(3), \tag{19}$$

$$\dot{z} = \delta z + br^2 - z^2 + \mathrm{O}(3), \tag{20}$$

so that $(r, z) = (0, 0)$ is a fixed point for all ε, δ; this corresponds to the fact that the trivial homogeneous state $(u, v) = (0, 0)$ is always a solution to the Brusselator equations. Note that the form (19) and (20) may always be converted to (17) and (18) by the transformation $z \to z + \frac{1}{2}\delta$, with corresponding changes in the definitions of the unfolding parameters ε and δ; so that the results from the saddle–node/Hopf studies referred to above may all be applied to the transcritical/Hopf case. In this paper, we give all results in the form appropriate to (19) and (20); they could equally well be derived for (17) and (18), as in the cited literature.

3.2. *Analysis of quadratic system*

Analysis of this system (Guckenheimer and Holmes, 1986; Chow et al., 1994) reveals that the behavior depends crucially on the signs of a and b. In all cases, the origin $(r, z) = (0, 0)$ is a fixed point, which becomes unstable via a transcritical bifurcation to another fixed point on the z-axis $(0, \delta)$ (we recall that this bifurcation corresponds to the Turing bifurcation in the full reaction–diffusion system). This fixed point may then undergo a further pitchfork bifurcation in the planar system, to give a nontrivial fixed point off the axis, at

$$(r, z) = \left(\sqrt{\frac{b\varepsilon}{a}\left(\frac{\varepsilon}{a} + \delta\right)}, -\frac{\varepsilon}{a} \right).$$

This secondary planar pitchfork corresponds to a Hopf bifurcation, and the ensuing fixed point to a periodic orbit, in the three-dimensional system.

So far this is as would be expected from naïvely coupling a transcritical and Hopf bifurcation. It is the further behavior that distinguishes the different cases. For some values of a and b nothing further happens, but of particular interest is the "case III" of Guckenheimer and Holmes (1986), in which $a > 0$, $b = -1$. In this case, the nontrivial steady state undergoes a Hopf bifurcation for $\delta > 0$, as ε increases through $-\frac{1}{2}a\delta$; in the full three-dimensional system, this corresponds to a Hopf bifurcation of the limit cycle to a torus (Langford, 1979). As noted by Scheurle and Marsden (1984), we thus find in a structurally stable unfolding the beginnings of the Landau sequence of bifurcations or "route to chaos":

		primary		
trivial	$\longrightarrow$	branch of	$\longrightarrow$ secondary branch	$\longrightarrow$ tertiary branch of
equilibrium		equilibria	of Hopf orbits	quasi-periodic 2-tori

However, the super- or sub-criticality of the Hopf bifurcation, and thus the stability of the resulting planar limit cycle (torus in the full system), is not determined by the quadratic terms in the normal form, for the relevant coefficient in the Hopf bifurcation vanishes (Marsden and McCracken, 1976; Guckenheimer and Holmes, 1986). Indeed, at $\varepsilon = -\frac{1}{2}a\delta$ the quadratic system is completely integrable: see (23).

This observation forms the basis for much of the subsequent analysis: The stability is undetermined by the 2-jet; *higher-order terms are needed for a generic unfolding*. It is thus essential to compute cubic terms in the normal form to determine the behavior of the system. However, while derivation and analysis of the quadratic normal form is fairly straightforward, the addition of cubic terms considerably adds to the analytical and computational difficulties.

3.3. The effect of a single cubic term

As an example of the effects of cubic terms, we follow Guckenheimer and Holmes (1986) and consider the simplest case, in which a single cubic term appears in the normal form:

$$\dot{r} = \varepsilon r + arz, \tag{21}$$

$$\dot{z} = \delta z + br^2 - z^2 + fz^3. \tag{22}$$

In fact, Guckenheimer and Holmes show that *any* third-order system of the form (7) may be reduced to this case, at the expense of further normal form transformations and a state-dependent change of time-scale, on which we shall comment further. The simplest approach, valid for small r, z, ε and δ, is to consider the cubic term as a perturbation of the quadratic normal form, and only study its effect on the Hopf bifurcation. After the linear transformation $\tilde{\varepsilon} = \varepsilon + \frac{1}{2}a\delta$ in (21) and (22) (so that the bifurcation occurs for $\tilde{\varepsilon} = 0$), we perform a "blowing up" rescaling

$$r = \sigma u, \quad z = \sigma v, \quad \tilde{\varepsilon} = \sigma \nu_1, \quad \delta = \sigma \nu_2, \quad t \to \sigma^{-1}\tau$$

to obtain the system

$$\dot{u} = \sigma \nu_1 u - \tfrac{1}{2}a\nu_2 u + auv, \qquad \dot{v} = \nu_2 v - u^2 - v^2 + \sigma f v^3.$$

This system now lends itself to Mel'nikov analysis; the unperturbed system ($\sigma = 0$) has integral

$$G(u, v) = \frac{a}{2}u^{2/a}\left[\nu_2 v - \frac{1}{1+a}u^2 - v^2\right], \tag{23}$$

and is Hamiltonian after a time rescaling. The Mel'nikov theory for small σ then indicates that a unique limit cycle persists for a range of $\nu_1 - \nu_2$ parameter values, and disappears on coalescing with the stable and unstable manifolds of (two of) the fixed points on the z-axis in a heteroclinic orbit. The demonstration of this result, especially the uniqueness of the limit cycle, involves fairly lengthy and complicated calculations, and was first completed rigorously by Zholondek (1984); see also Carr et al. (1985), van Gils (1985), Guckenheimer and Holmes (1986) and Chow et al. (1989). The stability of the limit cycle depends on the sign of f – it is stable for $f < 0$ for the system (21) and (22).

This analysis, along with elementary calculations of the codimension one bifurcations of (19) and (20) referred to earlier, yields the bifurcation diagram of Fig. 2 for the transcritical/Hopf unfolding. On this diagram, using the conventions of Guckenheimer and Holmes (1986) and Arnol'd (1988), we show the bifurcation curves of the planar system emanating from the degenerate codimension two point $\varepsilon = \delta = 0$, with a "cartoon" of the r–z phase portrait associated with each open sector of parameter space in the sector $\varepsilon < 0$, $\delta > 0$. This figure is an analytically derived, generic guide for analyses of specific systems.

3.4. Implications for three-dimensional system

The significance of the above results appears on considering their implications for the full three-dimensional system. In this case, the planar limit cycle corresponds to a two-torus, which is hyperbolic at least immediately after the bifurcation. The flow on this torus is doubly periodic, with fast frequency $\approx \omega$ and slow frequency $\approx O(\delta)$; if the rotation number (obtained from the ratios of the fast and slow frequencies) is rational, the flow is periodic, otherwise it is quasi-periodic and irrational (ergodic), and it may be shown that typically both situations occur, with ergodic flow arising for a set of parameter values of positive measure (Scheurle and Marsden, 1984).

As discussed in Guckenheimer (1981) and Guckenheimer and Holmes (1986), a generic vector field in $\mathbb{R}^3$ is not SO(2) symmetric, even though nonsymmetric terms may be removed to all orders in the normal form transformation.

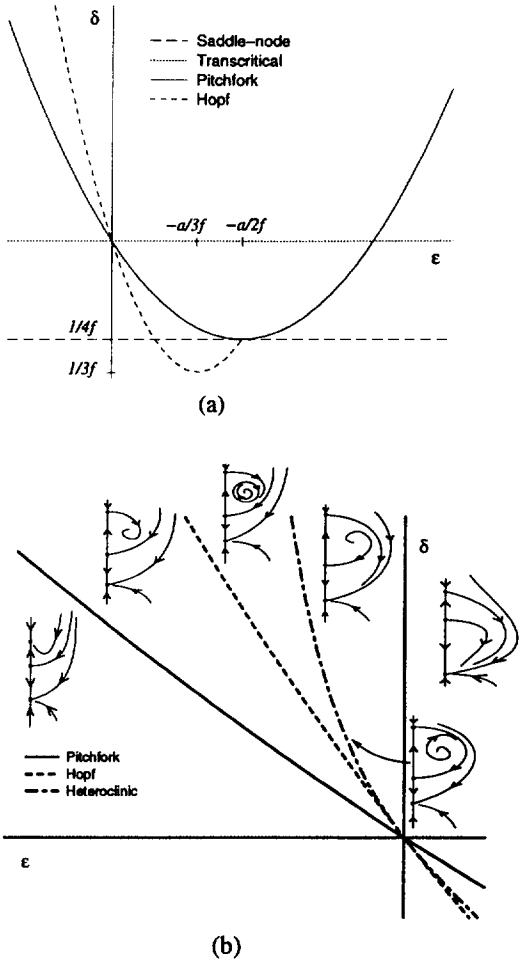

Fig. 2. Bifurcation diagram for transcritical/Hopf bifurcation with a single cubic term, (21) and (22), with $a > 0, b = -1, f > 0$: (a) partial diagram, showing elementary in full parameter space; (b) enlargement of region of interest, showing pitchfork, Hopf and heteroclinic curves (the separation between the Hopf and heteroclinic curves has been exaggerated for clarity).

In the absence of symmetry, the picture in Fig. 2 is perturbed. Since away from bifurcation points the torus is hyperbolic, it will persist for an open set of parameter values, but the dynamics on it will typically exhibit complicated intervals of phase-locking and irrational flow. This has been confirmed by the studies of Kirk (1991, 1993) on the structure of the resonance tongues which arise when the symmetry is broken by the (arbitrary) addition of low-order terms.

The planar Mel'nikov analysis also predicts the existence of a heteroclinic orbit connecting the two fixed points (0,0), $(0, \delta)$ for a curve of parameter values. In the three-dimensional system, this corresponds to a heteroclinic manifold: a sphere around the z-axis. However, in the absence of symmetry such a coincidence of two 2-manifolds in $\mathbb{R}^3$ is nongeneric, and we expect a splitting of these manifolds, leading to transverse intersections. Furthermore, a homoclinic orbit to a spiral saddle (a Šil'nikov connection) may be shown to occur, so that all the attendant complexity, including a countable number of horseshoes and chaos, may be expected for an open set of parameter value (see Glendinning and Sparrow (1984) and Guckenheimer and Holmes (1986)).

For the rest of this paper we shall be interested in seeking the parameter domain of existence of the torus, and the heteroclinic connection, which occur in the vicinity of the Hopf bifurcation in the normal form. Thus we restrict our attention to the sector $\varepsilon < 0, \delta > 0$ shown in Fig. 2(b), which is common to all systems of the form (7), as demonstrated by the bifurcation calculations in Section 5.4. The remaining features of Fig. 2(a) depend on the specific form of (21) and (22), and will not concern us any further.

3.5. Studies on the effects of cubic terms

The above predictions for the three-dimensional system in the absence of symmetry were initially made on the basis of a cubic perturbation from the quadratic normal form (Guckenheimer, 1981; Guckenheimer and Holmes, 1986). They have been verified and extended by a number of studies on the effects of cubic and higher terms. These confirm that the location and stability of the torus and homoclinic bifurcation are determined by the cubic terms in the normal form (that is, terms preserving the SO(2) symmetry and invariance of the z-axis), while the breakup of the torus and occurrence of the Šil'nikov homoclinic connection, with related (chaotic) dynamical behavior, depend on the breaking of the symmetry, even if this vanishes to all orders. Indeed, Broer and Vegter (1984) demonstrated the existence in generic unfoldings of this codimension two singularity, of subordinate Šil'nikov bifurcations of codimension one; they emphasized that this was a C^∞-flat phenomenon in the sense that it could be completely annihilated by a flat perturbation. Kirk (1991, 1993) discussed the need for the breaking of axisymmetry for the formation of complicated behavior, and demonstrated that the addition of certain nonsymmetric cubic terms to the normal form could lead to break-up of the torus and the associated creation and merging of resonance tongues; as well as heteroclinic tangencies and homoclinic bifurcations. Unfortunately, the cubic terms she added, seemingly arbitrarily chosen, do not coincide with those that survive in the normal form. It is therefore difficult to relate her findings to any specific system.

Gaspard (1993), in studying local birth of homoclinic chaos of Šil'nikov type, also recognized that this was due to the breaking of axisymmetry, as the resonant terms could not account for the origin of chaos; so he considered the effect of adding general cubic terms to the quadratic normal form. The calculations showed that the *condition* for homoclinic orbits, to finite order, depends only on the resonant cubic terms which survive in the normal form; but that the very *existence* of the homoclinic bifurcation depends on the nonresonant terms, although their contribution to the bifurcation curves is flat. An important aspect of his results for our calculation is the confirmation that while the torus and homoclinic/heteroclinic bifurcations coincide if we consider only the quadratic normal form, they are split by the inclusion of cubic terms, which furthermore serve to determine the stability of the torus. Since we seek complex dynamics near the region of existence of the torus, and use the normal form to determine this region, we need the cubic terms in order to detect this region in parameter space. Gaspard's formulae for the bifurcation curves will be given in Section 5.3, adapted to our particular transcritical/Hopf normal form and related to stability results for (21) and (22) mentioned earlier.

In summary, provided the conditions $a > 0, b = -1$ in the quadratic normal form are satisfied, normal form theory predicts the formation of a torus and, generically, break-up of this torus, involving homoclinic Šil'nikov connections and chaos. The existence of chaos depends on the breaking of axisymmetry; this occurs for our original differential equation, but is lost in the normal form analysis. However, the normal form can indicate the position and stability of the Hopf bifurcation leading to the torus, the region in parameter space in which the torus occurs, and the locus of the heteroclinic connection in the two-dimensional normal form, which differs by a flat function from the loci of the homoclinic Šil'nikov connections. These regions in parameter space (shown schematically in Fig. 2(b)), which we seek in the normal form in order to relate them to the original PDE or to the ODEs derived from it, depend necessarily on the cubic terms. Our next step is thus to calculate the cubic terms, and their coefficients.

4. Cubic normal forms

The classical theory (Arnol'd, 1982; Guckenheimer and Holmes, 1986), sketched in Appendix A, predicts the normal form:

$$\begin{aligned}\dot{r} &= a_1 rz + a_2 r^3 + a_3 rz^2 + \mathrm{O}(4),\\ \dot{z} &= b_1 r^2 + b_2 z^2 + b_3 r^2 z + b_4 z^3 + \mathrm{O}(4),\\ \dot{\theta} &= \omega + c_1 z + c_2 r^2 + c_3 z^2 + \mathrm{O}(3);\end{aligned} \tag{24}$$

from an analysis of resonant terms. Formulae for the coefficients a_j, b_j, c_j are given in Appendix A (Eqs. (A.5)–(A.14); also see (11)–(14)). It turns out, however, that there is some freedom in the transformations leading to (24): there are undetermined coefficients in the transformation for the quadratic terms that affect the coefficients of the cubic terms. The normal form is not unique, and may be simplified further; some of the *resonant* cubic terms may be removed. A full analysis of this situation, in which the "simplest" normal form is obtained by making use of information from nonlinear (quadratic, here) as well as the linear terms, was given by Ushiki (1984) (see also Chua and Kokubu (1988, 1989) for a more accessible account). Unfortunately, the methods given in these works for determining the simplest possible structure of the normal form are not very helpful for computing its coefficients, although they confirm that the results developed below are in fact the simplest possible.

Before dealing with the cubic terms, we note that we wish not only to calculate a universal unfolding, but also to retain the correspondence between the unfolding parameters ε and δ, to enable comparisons and predictions. Thus we must calculate the normal form not merely for (7), but for a more general system, in which ε and δ enter in the most general way consistent with the singularity, while reducing to (7) for $\varepsilon = \delta = 0$. By suitable choice of ε and δ as perturbations of the bifurcation parameters of the original system (see Appendix B, Eqs. (B.9) and (B.10)), our system may be written in the form

$$\begin{aligned}\dot{x} &= \varepsilon x - (\omega + \omega_\varepsilon \varepsilon + \omega_\delta \delta) y + f(x, y, z, \varepsilon, \delta),\\ \dot{y} &= (\omega + \omega_\varepsilon \varepsilon + \omega_\delta \delta) x + \varepsilon y + g(x, y, z, \varepsilon, \delta),\\ \dot{z} &= \delta z + h(x, y, z, \varepsilon, \delta).\end{aligned} \tag{25}$$

We shall work throughout to first order in ε and δ. As shown in Appendix A, the truncated cubic normal form for this system (after some of the cubic coefficients in the $\dot{z}$ equation have already been chosen to vanish) is

$$\dot{r} = \varepsilon r + (a_1 + \alpha_1 \varepsilon + \alpha_2 \delta) rz + a_2 r^3 + a_3 rz^2, \tag{26}$$

$$\dot{z} = \delta z + b_1 r^2 + b_2 z^2 + b_3 r^2 z + b_4 z^3, \tag{27}$$

$$\dot{\theta} = \omega + \omega_\varepsilon \varepsilon + \omega_\delta \delta + (c_1 + \gamma_1 \varepsilon + \gamma_2 \delta) z + c_2 r^2 + c_3 z^2, \tag{28}$$

where, in addition, two of a_2, a_3 and b_3 may also be chosen to vanish, as may one of c_2 and c_3. The full expressions for the coefficients in the minimal normal form obtained by choosing a_3, b_3 and c_3 to be zero, are listed in Appendix A, Eqs. (A.28)–(A.34).

4.1. The three types of normal form

As in (15) and (16), we may further simplify the above expression by the rescaling (A.37) given in Appendix A. The $\dot{\theta}$ equation decouples, and does not affect the dynamics of the other equations, and so we consider only the $\dot{r}$ and $\dot{z}$ equations, obtaining three different types of normal form, corresponding to retaining one of the cubic coefficients a_2, a_3 or b_3. We shall compare the usefulness of these three types later, and hence list them here:

Type I (keeping $r^3\partial/\partial r$):

$$\dot{r} = \varepsilon r + (a + \kappa\varepsilon + \lambda\delta)rz + gr^3, \qquad \dot{z} = \delta z - r^2 - z^2 + fz^3. \tag{29}$$

Type II (keeping $rz^2\partial/\partial r$):

$$\dot{r} = \varepsilon r + (a + \kappa\varepsilon + \lambda_{\mathrm{II}}\delta)rz + hrz^2, \qquad \dot{z} = \delta z - r^2 - z^2 + fz^3. \tag{30}$$

Type III (Keeping $r^2z\partial/\partial z$):

$$\dot{r} = \varepsilon r + (a + \kappa\varepsilon + \lambda\delta)rz, \qquad \dot{z} = \delta z - r^2 - z^2 + er^2z + fz^3. \tag{31}$$

Appendix A gives relations between e, g and h, and also between λ and λ_{II}, in Eqs. (A.38)–(A.39).

4.2. *Simpler systems related to the normal form*

As discussed in Appendix A, a transformation of the time variable $\tau = (1 + \nu z)^{-1}t$ with suitably chosen ν, enables a further term to be removed from the above cubic normal forms. Retaining only the $z^3\partial_z$ term, we may thus consider a system of the form

$$\frac{\mathrm{d}r}{\mathrm{d}\tau} = \varepsilon r + (a + \tilde{\kappa}\varepsilon + \tilde{\lambda}\delta)rz, \qquad \frac{\mathrm{d}z}{\mathrm{d}\tau} = \delta z - r^2 - z^2 + \tilde{f}z^3; \tag{32}$$

where expressions for $\tilde{f}$, $\tilde{\kappa}$ and $\tilde{\lambda}$ in terms of f, g, κ and γ are given in (A.43). This is essentially what was done in Guckenheimer and Holmes (1986) to obtain (21) and (22).

Finally, for our numerical experiments we retained ε and δ in the more general form (25) rather than just (7), as has usually been considered in the literature. To investigate whether this more general form is necessary, we may calculate the bifurcation diagram for one of the normal forms obtained above *without* including the higher-order ε–δ dependence (this amounts essentially to setting $\kappa = \lambda = 0$), specifically the equivalent of type I (the others yield similar results)

$$\dot{r} = \varepsilon r + arz + gr^3, \qquad \dot{z} = \delta z - r^2 - z^2 + fz^3. \tag{33}$$

Equipped with all the above normal forms and derived systems, and with the expressions of Appendix A for the coefficients in these systems, we now return to study the transcritical/Hopf bifurcation in the Brusselator.

5. Application to the Brusselator

Before carrying out the normal form analysis on the Brusselator, several preliminary calculations are needed to reduce the PDE first to a system of ODEs, then to restrict to a three-dimensional ODE, from which in turn the normal form may be derived. These calculations, and the approximations inherent in them, are discussed briefly here and in more detail in Appendix B.

As already mentioned in Section 2.1, the PDE is recast as a system of ODEs by Galerkin projection onto Fourier sine modes which respect the boundary conditions. This yields the infinite system of ODEs (B.2) and (B.3) for the time evolution of the modal amplitudes β_k and γ_k. The nonlinearity couples all distinct modes, but the linear terms are uncoupled, that is, the linear evolution of β_k for a given k (and similarly that of γ_k) depends only on β_k and γ_k, and not on β_l or γ_l, $l \neq k$. The Fourier representation of the Laplacian operator therefore diagonalizes in 2×2 blocks. The Jacobian matrix which determines linear stability of the lth mode has already been quoted (2).

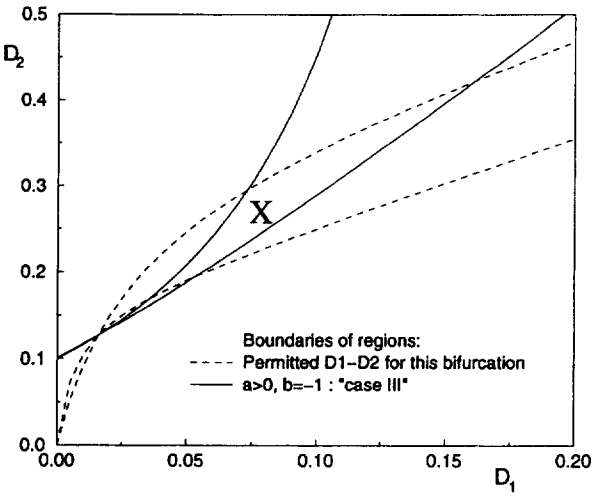

Fig. 3. Admissible D_1–D_2 range for the transcritical/Hopf bifurcation for $k = 3$ (dashed curves), and boundary of region (solid curves) for which $a > 0, b = -1$, i.e. a "case III" bifurcation occurs. We choose parameters in the region marked X, in which both sets of conditions are satisfied.

The transcritical/Hopf bifurcation from the trivial equilibrium occurs when for certain parameter values there is a pair of pure imaginary eigenvalues in the stability matrix for one mode, a single zero eigenvalue in another, and all other eigenvalues are negative, that is, the zero equilibria for all other amplitudes are stable. We note that since trace(E_l) is monotonically decreasing in l, a pair of imaginary eigenvalues in any mode $l > 1$ implies instability in mode 1; hence the Hopf bifurcation must occur in the first mode. Thus, following Guckenheimer (1981), for

$$B = B_c \equiv 1 + A_c^2 + D_1 + D_2, \qquad A^2 = A_c^2 \equiv D_2 k^2 \frac{D_1 + D_2 - D_1 k^2}{1 + k^2(D_1 - D_2)}, \tag{34}$$

it can be checked that a Hopf bifurcation in mode 1 is coupled to a transcritical (Turing) bifurcation in the kth mode; all other eigenvalues being negative if $\det(E_{k\pm1}) > 0$ (see Appendix B, (B.7) and (B.8) for detailed conditions). This condition significantly restricts the possible parameter domains for D_1 and D_2 for this bifurcation to occur. See Fig. 3 for a plot of the admissible domain for $k = 3$, bounded by dashed curves (in fact, only conditions (B.8) are shown; for $D_1 > 1/63$, (B.7) are satisfied if (B.8) are). It turns out that due to the way the modes interact (see (B.4)) that even k gives vanishing quadratic terms in the normal form, and the lowest nonzero terms are cubic. We do not study this more degenerate situation here, see Holmes (1980, 1981), and thus suppose k to be odd. This implies that for our choice of parameter values, the (invariant) odd subspace will be stable and asymptotically attracting, i.e. all even modes decay.

It is convenient to perform a linear transformation within each mode, $(\beta_k, \gamma_k) \to (\tilde{\beta}_k, \tilde{\gamma}_k)$, to diagonalize the ODEs while putting mode 1 into the canonical rotation form. This change of coordinates applied to (B.2) and (B.3) thus yields a system which has linearization at the bifurcation point

$$\begin{pmatrix} 0 & -\omega & 0 & 0 \\ \omega & 0 & 0 & 0 \\ 0 & 0 & 0 & 0 \\ 0 & 0 & 0 & T \end{pmatrix}, \tag{35}$$

where $\omega = \det(E_1)$ and all eigenvalues of the operator T, corresponding to the stable modes, have negative real parts.

When we perturb B and A from their bifurcation values B_c and A_c (34), the linearization changes, but with suitably chosen ε and δ as linear combinations of $B - B_c$ and $A^2 - A_c^2$, the perturbed system restricted to the three critical (center) modes still has the block-diagonal linearization

$$\begin{pmatrix} \varepsilon & -\omega(\varepsilon,\delta) & 0 \\ \omega(\varepsilon,\delta) & \varepsilon & 0 \\ 0 & 0 & \delta \end{pmatrix}, \tag{36}$$

where $\omega(\varepsilon,\delta) = \omega + \omega_\varepsilon \varepsilon + \omega_\delta \delta$. The relevant definitions of ε and δ are given in (B.9) and (B.10), with the numerical values for the parameter values we consider cited in (39) and (40).

The next step is to project the (infinite) system onto the three center modes, using either a tangent space approximation (essentially a truncation, which ignores all modes except the critical ones), or more generally by calculating an approximation to the center manifold and substituting this into the equations to obtain an improved approximation to the flow restricted to the center manifold, as sketched in Section 2.2. Since the center manifold is tangent to the space spanned by the critical modes at the origin (that is, the approximation to the center manifold is at least quadratic) and the interaction between the modes is nonlinear, the higher modes only affect the dynamics of the critical modes at cubic order. Hence the calculation of the quadratic terms in the normal form, which we discuss next, is unaffected by our choice of projection, but we must consider a quadratic center manifold in the calculation of cubic terms in Section 5.2.

5.1. *Parameter values and quadratic normal form*

5.1.1. *Formulae for quadratic coefficients*

The calculations for the quadratic coefficients in the normal form for the transcritical/Hopf bifurcation for the Brusselator have been reported elsewhere (Guckenheimer, 1981, 1984; Scheurle and Marsden, 1984), and are summarized in Appendix B: see Eqs. (B.11)–(B.13). From these formulae it is evident that, as noted above, the quadratic coefficients vanish if k is even; so we will only consider the less degenerate case of interaction between the 1st and kth mode, where k is odd. The coefficients cited in the appendix are not unique, as they depend on the choice of scaling for r and z; as in the passage to (15) and (16), we rescale r and z to get the (unique) coefficients a and b in the rescaled normal form. We may write down these coefficients for the Brusselator:

$$a = \frac{3(k^2-1)}{k^2(k^2-4)} \frac{(A^2(1+k^2(D_1+D_2)) - k^2 B D_2)(D_1+D_2)}{(2A^2(1+k^2 D_1) - k^2 B D_2) D_2}, \tag{37}$$

$$b = -\operatorname{sign}[(2A^2(1+k^2 D_1) - B k^2 D_2)(1 + D_1 - D_2) \times (1 + D_1 - D_2 - A^2)(k^2-4) D_2] = \pm 1, \tag{38}$$

where $k (k > 1$, odd) is the mode number of the mode with the zero eigenvalue, and A and B are as defined in (34).

The discussion in Section 3 indicates that the "interesting" behavior for this bifurcation occurs when $a > 0, b = -1$. Applying these conditions to (37) and (38) on substituting the bifurcation B and A^2 values (34) gives further necessary and sufficient conditions on D_1 and D_2 for this bifurcation, shown bounded by the solid curves in Fig. 3, in addition to the constraints (B.7) and (B.8) mentioned above and in Appendix B. For any given k, there is a restricted, but open, parameter domain in which we obtain the "interesting" behavior, including torus creation and Šil'nikov chaos. The ranges of D_1–D_2 parameter values yielding the bifurcation of interest for $k = 3$ are indicated by region X of Fig. 3.

5.1.2. Guckenheimer's parameter choice

Guckenheimer (1981) recognized that there are parameter values D_1, D_2 for which the transcritical/Hopf bifurcation occurs with $a > 0, b = -1$; he proposed the values (also cited in Guckenheimer (1984) and Scheurle and Marsden (1984))

$$k = 5, \quad D_1 = 0.02, \quad D_2 = 0.09$$

(which satisfy (B.7) and (B.8)) so that

$$B_c = 2.28, \quad A_c^2 = 1.17, \quad \omega = 1.03923.$$

In this case the rescaled quadratic coefficients (37) and (38) in the normal form are

$$a = 0.0768254, \quad b = -1.$$

It was on the basis of these values and the theory in Section 3 that Guckenheimer was able to conclude the presence of chaos in the Brusselator, appealing to mild genericity assumptions, without actually computing higher-order terms.

Our initial goal was to confirm Guckenheimer's results by extending his normal form calculations to third order (the necessity for which we have already seen) and detecting the chaos. It turns out, unfortunately, that Guckenheimer's parameter values yield cubic coefficients ranging over several orders of magnitude, and extremely narrow parameter domains for the bifurcation. We therefore sought alternative parameter values, for which the numbers were not quite as bad, and for the rest of this paper we analyze that case. Some of the analogous results for Guckenheimer's parameter choice are reported for comparison in Appendix C.

As these results indicate, the interaction between mode 1 and mode 5 yields very narrow parameter domains of interest, in addition to relatively large influences in the center manifold from other modes, in particular the intermediate mode 3. It seems plausible that a lower critical mode would give better results. The even modes 2 and 4 yield a more degenerate situation, as already discussed; so we were prompted to consider interactions between modes 1 and 3, provided parameter values for D_1 and D_2 exist which give the desired unfolding. That such values exist is demonstrated by the region of Fig. 3 marked by X.

5.1.3. Improved parameter values

For $k = 3$, acceptable parameter values are $D_1 = 0.10$, $D_2 = 0.30$, which satisfy all the requirements. If A and B are chosen as in (34), there is a pair of pure imaginary eigenvalues in mode 1, a zero eigenvalue in mode 3, and all other modes are stable. The remaining parameter values, and the Hopf bifurcation frequency, are

$$B_c = 3.0875, \quad A_c^2 = 1.6875, \quad \omega = 1.122497.$$

The quadratic coefficients in the normal form are

$$a_1 = -0.1218437, \quad b_1 = 0.0150555, \quad b_2 = 0.5745019,$$

which give after rescaling

$$a = 0.21208577, \quad b = -1;$$

the desired "case III" unfolding. We retain these values of D_1 and D_2 for the rest of the paper; other parameter values in region X of Fig. 3 appear to yield qualitatively similar results.

It is interesting to note that other types of unfoldings in the Guckenheimer and Holmes (1986) classification may be obtained by varying the parameters, for instance, varying D_2 for fixed D_1, while all other conditions for

Table 1
Eigenvalues in lowest odd modes (the largest eigenvalues in modes 2 and 4 are −0.45000 and −0.36324, respectively)

Mode	Eigenvalues	
1	1.122497 i	−1.122497 i
3	0	−3.2
5	−1.05300	−8.54700
7	−3.20782	−15.9922
9	−6.27683	−25.7232
11	−10.2000	−37.8000

this bifurcation remain satisfied. (This amounts to staying in the "permitted" régime satisfying (B.7) and (B.8) (see Fig. 3), while moving out of the "$a > 0, b = -1$" régime.) The type of the unfolding is given by the signs of the rescaled parameters a and b; for example:

$$D_1 = 0.10,\ D_2 = 0.26 \ \Rightarrow\ a = +1.661927,\ b = +1, \quad \text{case I};$$
$$D_1 = 0.10,\ D_2 = 0.28 \ \Rightarrow\ a = -0.504381,\ b = -1, \quad \text{case IV}.$$

For our chosen parameter values $D_1 = 0.10$, $D_2 = 0.30$, the eigenvalues in the lowest odd modes are given in Table 1. As the eigenvalues decay quite rapidly, the higher (odd) modes are increasingly stable, and we would expect them to have increasingly little effect on the dynamics of the center manifold. The assumption is supported by the calculation of normal form coefficients after including successively more terms in the center manifold (see Table 2), and the accuracy of the Galerkin projection including modes up to mode 7 in representing the full PDE near the bifurcation (see Fig. 4).

The appropriate definitions of the unfolding parameters ε and δ in terms of the perturbations in B and A^2 from their bifurcation values are found by substituting the parameter values into the definitions (B.9) and (B.10) to yield:

$$B = B_c - (19/4)\varepsilon + 4\delta, \quad B_c = 3.0875, \tag{39}$$
$$A^2 = A_c^2 - (27/4)\varepsilon + 4\delta, \quad A_c^2 = 1.6875. \tag{40}$$

5.2. *Center manifold reduction and the cubic normal form*

For the calculation of the quadratic terms for the reduced three-dimensional dynamics, and hence the normal form, we merely needed to truncate to the space spanned by the critical modes. However, the reduced dynamics properly occur on the center manifold, which has a quadratic tangency with the tangent space; so the stable, decaying modes influence the dynamics on the center manifold at cubic and higher orders.

5.2.1. *Center manifold projection – general description*

The general principle of center manifold reduction was outlined in Section 2.2. For the present calculation, since the higher (odd) modes only influence the dynamics of the stable modes through quadratic terms in the Galerkin projection (see (B.2)–(B.5)) we need only to calculate the center manifold approximation $h(x)$ to lowest, quadratic order to obtain a center manifold accurate to cubic order.

In principle *all* odd modes contribute to the center manifold calculation. However, since the modes become increasingly stable (as demonstrated by Table 1) it is likely that only the lowest few will affect the dynamics to the precision we are interested in; higher modes are expected to decay fast enough that they essentially do not contribute, and numerical evidence appears to confirm this. The approach we used to determine how many modes are relevant, was to recalculate the cubic normal form coefficients using successively more modes; when the addition of extra

Table 2
Effect of including successively more modes in the center manifold, for the type I normal form

Modes	f	g	κ	λ
TS	−44.1621	−10.7764	5.32294	−34.8397
5	−37.8767	−10.0777	5.19038	−34.8501
7	−36.9532	−10.0987	5.19038	−34.8209
11	−36.9247	−10.0999	5.19038	−34.8190
21	−36.9239	−10.0999	5.19038	−34.8189

modes ceased to alter the coefficients to the desired accuracy, we felt justified in neglecting them. In other cases with simpler nonlinear terms it is possible to verify this analytically (e.g., Armbruster et al. (1989)).

5.2.2. Number of modes included

The center manifold reduction was performed as outlined in (4) and (5), to calculate a quadratic approximation to the graph $h(x)$ for the odd stable modes. This approximation was substituted into the dynamical equations (B.2) and (B.3) for the critical modes, to obtain a system of three ODEs, of the form (25), on the center manifold. Using the formulae for the normal form coefficients listed in Appendix A, and rescaling, we found the normal form coefficients for the normal forms types I, II and III (29)–(31). We used the coefficients for the type I normal form listed in Table 2 to gauge the effect of the higher, stable modes. Odd modes up to the 21st were added. Here TS denotes the tangent space truncation.

The normal form coefficients settle down quite rapidly, and cease to change within the precision of our calculations well before inclusion of mode 21, as indicated by Table 2; hence we take the normal form coefficients derived from a center manifold computed from 21 odd Galerkin modes (a 22-dimensional system) as the "exact" values. Indeed, the inclusion of all odd modes up to 7 (that is, eight equations in total, since we have two equations per mode, for β and γ, corresponding to the two state variables u and v) already appears to give a very good approximation to the center manifold, with the coefficients differing from the "exact" values by less than one part in 10^3. This observation, in fact, motivates the study of the full PDE using an eight-equation Galerkin projection, to which we shall return later.

Performing this reduction, we obtain the equations, up to cubic order, on the center manifold, and then use these equations and the formulae in Appendix A to calculate the normal forms. For $k = 3$, $D_1 = 0.10$, and $D_2 = 0.30$, these are:

Type I (keeping $r^3\partial/\partial_r$):

$$\begin{aligned} \dot{r} &= \varepsilon r + (0.2120858 + 5.190383\varepsilon - 34.818885\delta)rz - 10.099903r^3, \\ \dot{z} &= \delta z - r^2 - z^2 - 36.923864z^3. \end{aligned} \tag{41}$$

Type II (keeping $rz^2\partial/\partial r$):

$$\begin{aligned} \dot{r} &= \varepsilon r + (0.2120858 + 5.190383\varepsilon - 47.060833\delta)rz + 12.241948rz^2, \\ \dot{z} &= \delta z - r^2 - z^2 - 36.923864z^3. \end{aligned} \tag{42}$$

Type III (keeping $r^2z\partial/\partial z$):

$$\begin{aligned} \dot{r} &= \varepsilon r + (0.2120858 + 5.190383\varepsilon - 34.818885\delta)rz, \\ \dot{z} &= \delta z - r^2 - z^2 - 115.443372r^2z - 36.923864z^3. \end{aligned} \tag{43}$$

As indicated in Section 4, for comparison, we also study the system (32) following the time transformation, and the system (33) ignoring the higher-order ε–δ dependence. The former is found from (41) via the transformations (A.43), to give

$$\begin{aligned} \dot{r} &= \varepsilon r + (0.2120858 - 33.290740\varepsilon - 51.141482\delta) rz, \\ \dot{z} &= \delta z - r^2 - z^2 + 1.557259 z^3. \end{aligned} \tag{44}$$

For the latter system, we simply drop the κ and λ terms from (41), to obtain

$$\dot{r} = \varepsilon r + 0.2120858 rz - 10.099903 r^3, \qquad \dot{z} = \delta z - r^2 - z^2 - 36.923864 z^3. \tag{45}$$

Before continuing, we note briefly that the three types of normal form (41)–(43) may exhibit different "global" behaviors. For instance, a simple trapping region argument appealing to the dominant negative cubic terms shows that the type I system is always globally stable, while in the type II and III systems (depending on parameter values) blow-up can occur, in which $r \to \infty$ while z approaches a fixed point. This is essentially irrelevant for us, however, since we are only interested in the local behavior near the origin, in both r–z and ε–δ space, where the dynamics of the three normal forms are similar, as evidenced by the bifurcation results presented below.

5.2.3. Validity of normal form transformations

To investigate the apparent paradox of ostensibly equivalent normal forms exhibiting different global behaviors, we examined the normal form transformations (A.4) themselves. In the notation of (6), an obvious necessary condition for validity of the transformations is that $(I + Dk(z))$ be invertible. For our choice of parameter values, we have computed the minimum size of a ball in $\mathbb{R}^3$ for which (A.4) fails to be invertible, and have obtained the estimate that, for $\varepsilon = \delta = 0$ and in real Cartesian coordinates, the transformation leading to (41) is invertible for $x^2 + y^2 + z^2 \leq (0.173)^2$, with similar results for the transformations to other normal form types. Outside this ball, we cannot expect any connection between the normal forms and the original vector field, or with each other, and are thus not surprised by the discrepancies in global behavior noted above. All the bifurcation phenomena we consider in this paper occur safely within this radius of invertibility. However, we expect that the normal form ceases to be a useful representation of the original vector field well before the transformation loses invertibility, namely when neglected terms become comparable to those retained. A quantitative analysis of this is daunting, as it requires at least the estimation of the neglected terms, but we expect that the normal form loses its relevance for the full system far nearer the origin in state and parameter space. The bifurcation results presented below support this expectation.

5.3. Systems for comparison

On the basis of the general transcritical/Hopf bifurcation theory outlined in Section 3, we may utilize the above normal forms (41)–(43), and the simplified systems (44) and (45), to predict ε–δ parameter ranges of "interesting" behavior, in particular the bifurcation to the torus and the heteroclinic bifurcation with associated Šil'nikov homoclinic behavior. How useful are such predictions; specifically, how close are the bifurcation parameter values to those obtained in the "full" system?

We will compare the normal forms and "full systems" by computing those bifurcation curves that may be found in both cases, in ε–δ space. A comparison of the positions of the bifurcating orbits in phase space (r–z for the normal forms, higher-dimensional in the other cases) gives additional information, but is more complicated to carry out. The frequencies at (Hopf) bifurcation may also be compared; but in Section 5.4 we focus on the comparison of bifurcation curves. Before doing this, we summarize the systems to be compared.

5.3.1. Center manifold system

Recall that the normal forms are obtained via near-identity changes of variables performed on the three ODEs approximating the dynamics on the center manifold. Each normal form thus further approximates these ODEs near the bifurcation point, and we may compare its behavior with that of the reduced dynamical system from which it is

obtained. This latter system is obtained by Galerkin projection, linear transformation to diagonalize, and a center manifold projection including all odd modes up to the 21st; and truncated to cubic order, as described in Sections 5.1 and 5.2. We denote it by CM.

5.3.2. Galerkin projection

These center manifold equations are in turn only an approximation of the full Brusselator PDE dynamics, and to obtain a closer estimate of the true solutions we appeal to Galerkin and finite difference schemes. Galerkin projection to Fourier models is particularly appropriate here, since we work in the odd subspace and so only odd modes need to be considered. The coefficients listed in Table 2 suggest that modes up to 7 give a good approximation to the full dynamics, while yielding a system small enough to remain computationally tractable. Thus we project the Galerkin equations (B.2) and (B.3) onto the lowest odd modes, for $l = 1, 3, 5$ and 7, to get a system of eight ODEs representing the full PDE dynamics; we denote this eight-dimensional Galerkin projection system by GP.

5.3.3. Finite difference approach

We also choose a fundamentally different approach to solving the PDE, for independent verification that there is no systematic problem with the Galerkin approach: we use a finite difference scheme for the solution of (1), with an approximation for the spatial derivative. It turns out that this approximation needs to be done with some care, and that a standard second-order finite difference scheme is insufficient.

Fig. 4 shows the steady solution $u(\xi, t)$ to the Brusselator equations (corresponding to the fixed point at $(0, \delta)$ in the normal form), approximated both with the eight-ODE Galerkin truncation GP discussed above, and with several finite difference approximations (for $\delta = 0.006$; smaller δ values yield similar results). That the Galerkin solution is the most accurate for the PDE is demonstrated by the fact that increasingly accurate finite difference schemes successively approach GP; thus we shall take GP as representing the "full" PDE. Fig. 4(a) shows that the usual second-order finite difference scheme, taken on a grid of 20 points, is not very accurate; refining the discretization to one over 40 points improves the solution, but is still not satisfactory. We need to implement at least a fourth-order finite difference scheme; and as Fig. 4(b) shows, this is much closer to the Galerkin projection solution, and best over a 40 point grid. Our choice of finite difference scheme for the solution of (1), which we denote by FD, is thus a fourth-order scheme with the interval $(0, \pi)$ divided into 40 intervals, with appropriate fourth-order choice of boundary conditions; in total, with 39 interior points and two state variables u and v, this leads to 78 simultaneous differential equations. We comment further on the accuracy of finite difference schemes in Section 5.4.

5.3.4. Analytical formulae

In addition to the three systems discussed above, we may also compare results of the normal form bifurcation computations to analytical expressions for bifurcation curves; these curves being given by next-order corrections to those for the quadratic normal form mentioned in Section 3. The pitchfork bifurcation curves for the normal forms (41)–(43) (corresponding to Hopf in the full system) are relatively straightforward to calculate exactly, the simplest method being to calculate the stability of the upper fixed point on the z-axis (corresponding to the fixed point $(0, \delta)$ in the quadratic normal form) for $\delta > 0$; the pitchfork bifurcation occurs when this fixed point becomes unstable, spawning an off-axis fixed point.

The Hopf bifurcation curve in the normal forms (torus bifurcation in full system) is more difficult to obtain, as it requires a stability computation for the off-axis fixed point, and ultimately leads to a cubic equation for $\varepsilon(\delta)$, and the heteroclinic bifurcation is even more complicated. However, at this point we can appeal to the perturbation calculations of Gaspard (1993), who analyzed the effect of cubic terms on the location of the Hopf and homoclinic curves. The latter calculation is based on a Mel'nikov type analysis, matching stable and unstable manifolds, and

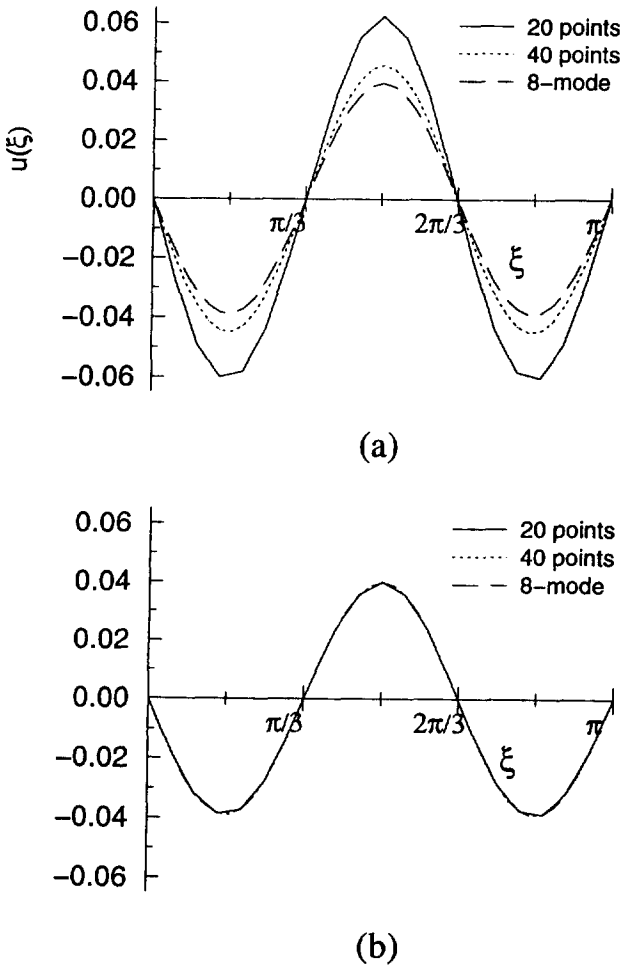

Fig. 4. Comparison between finite difference and 8-mode Galerkin schemes for computing a given fixed point for $\varepsilon = 5\times 10^{-6}$, $\delta = 0.006$: (a) Second order FD; (b) fourth order FD, both on 20 and 40 points grids. This shows clearly the inadequacy of the second order finite difference scheme, and the supremacy of the Galerkin method for this problem.

the results are given to lowest nontrivial order in the unfolding parameters. We have adapted all Gaspard's formulae to the case of the transcritical/Hopf bifurcation and to our parameter definitions (he gives them for the saddle–node/Hopf bifurcation) and we give them to quadratic order in δ, as functions $\varepsilon(\delta)$. For the general cubic normal form (A.35) and (A.36) we have:

$$\text{Hopf:}\quad \varepsilon = -\tfrac{1}{2}a\delta - \delta^2\left\{\tfrac{3}{8}af + \tfrac{1}{2}\lambda + \tfrac{1}{4}h - \tfrac{1}{4}a\kappa + \tfrac{1}{4}\left[(a+1)g + \tfrac{1}{2}ae\right]\right\} + \mathrm{O}(\delta^3) \tag{46}$$

$$\text{Heteroclinic:}\quad \varepsilon = -\tfrac{1}{2}a\delta - \delta^2\left\{\tfrac{3}{8}af + \tfrac{1}{2}\lambda + \tfrac{1}{4}h - \tfrac{1}{4}a\kappa + \frac{1}{4(3a+2)}\left[ah + \tfrac{3}{2}a^2 f + 2(a+1)^2 g + a(a+1)e\right]\right\} + \mathrm{O}(\delta^3). \tag{47}$$

Note that the linear terms $-\frac{1}{2}a\delta$ are identical for the Hopf and heteroclinic curves, and follow from the (integrable) quadratic normal form, as discussed in Section 3; the cubic terms split the bifurcation curves.

As we have discussed in Section 4 and Appendix A, two of e, g and h may be removed in (A.35) and (A.36), to give one of the minimal normal forms of types I, II or III (29) and (31). Thus the above formulae may be simplified for each of the three types of normal form. As expected, the formulae (46) and (47) are the same for all three types, if we take into account the relations (A.38) and (A.39) between the coefficients for the different normal forms. This happily confirms that the normal forms are all equivalent to order δ^2.

5.3.5. Stability criterion

Gaspard's formulae (46) and (47) for the bifurcation curves also enable us to deduce a stability criterion for the limit cycle obtained after the Hopf bifurcation, and for the heteroclinic cycle present in the normal form. We study the bifurcation behavior for fixed δ, increasing ε; compare Fig. 2(b). As ε increases, the off-axis fixed point in the normal form is created through a pitchfork bifurcation at $\varepsilon_{\mathrm{PF}}(= -a\delta$ to lowest order), and then becomes unstable through a Hopf bifurcation at $\varepsilon_{\mathrm{Hopf}}(= -\frac{1}{2}a\delta$ to lowest order). If the Hopf bifurcation is super-critical, then stable limit cycles exist for $\varepsilon > \varepsilon_{\mathrm{Hopf}}$, and are annihilated by collision with the heteroclinic cycle at $\varepsilon_{\mathrm{Het}} > \varepsilon_{\mathrm{Hopf}}$; this situation is shown in Fig. 2(b). Conversely, $\varepsilon_{\mathrm{Het}} < \varepsilon_{\mathrm{Hopf}}$ indicates a sub-critical Hopf bifurcation, for which unstable limit cycles exist for $\varepsilon < \varepsilon_{\mathrm{Hopf}}$ and collide with an unstable heteroclinic cycle; this case corresponds to unstable tori in the full system.

It is immediately apparent from (46) and (47) that $\varepsilon_{\mathrm{Hopf}} - \varepsilon_{\mathrm{Het}} = \mathrm{O}(\delta^2)$; this scaling will have important consequences for us later, in evaluating the likelihood of detecting the torus. The stability of the torus is found from the sign of $\varepsilon_{\mathrm{Hopf}} - \varepsilon_{\mathrm{Het}}$, and is of course independent of our choice of type of normal form. Expressed in terms of the coefficients of the normal form type I (29), we find

$$\varepsilon_{\mathrm{Hopf}} < \varepsilon_{\mathrm{Het}} \quad \text{if } 3af - 2(a+1)g < 0. \tag{48}$$

Satisfaction of the above inequality thus means that, near the bifurcation point, in the normal form a stable limit cycle (stable torus in the full system) is born out of a super-critical Hopf (secondary Hopf) bifurcation, and conversely.

For the Brusselator system with $k = 3$ and other parameter values as above, we find $3af - 2(a+1)g = 0.990816 > 0$, so that $\varepsilon_{\mathrm{Hopf}} > \varepsilon_{\mathrm{Het}}$ and the Hopf bifurcation is predicted to be sub-critical, leading to unstable limit cycles. For the PDE, this means that although quasi-periodic (two-frequency) solutions exist, they are unstable, and hence unlikely to be detected numerically, although they may play an important role in phase space as basin boundaries, separating solutions with distinct asymptotic behaviors. In addition, the difficulty in detecting the torus also depends on sizes of parameter ranges, as discussed in Section 5.4.

5.4. Bifurcation diagrams

Having described our various discretizations and approximations to the Brusselator dynamics at the transcritical/Hopf bifurcation point, we now compare them to establish the usefulness of normal forms in predicting the bifurcations and dynamics of the full system, in particular, torus creation and chaos. Here we compare the pitchfork and Hopf bifurcation curves in the planar normal forms to the corresponding primary and secondary Hopf bifurcation curves in the center manifold (CM), eight-dimensional Galerkin (GP), and finite difference (FD) systems. For the planar normal forms, we can also find an approximation to the heteroclinic bifurcation curve; its position relative to that of the Hopf curve in the normal form gives an indication, for the larger systems, of where the torus should exist and where chaos might occur.

5.4.1. Description of calculations

Bifurcation calculations were largely performed using AUTO94 (Doedel and Wang, 1994), with Maple used for analytic computations. In some cases, especially for the Hopf bifurcation, we could have used AUTOs facility

for two-parameter continuation of bifurcation curves, but such continuation is not always possible, e.g. for computing the torus bifurcation curves for systems of dimension three or more. Hence we chose to compute all curves point by point. Specifically, 10 different values of δ between 0.0001 and 0.004 were chosen, and bifurcation points for each fixed δ were computed using ε as the bifurcation parameter. For each set of computations, for an initial value of ε, an accurate fixed point (corresponding to the point $(0, \delta)$ in the quadratic normal form) was found as a starting point for the AUTO calculations. From this point, we continued in ε using AUTO.

In the planar normal forms (41)–(43) and related systems (44) and (45), the fixed point on the z-axis undergoes a pitchfork bifurcation at $\varepsilon_{\mathrm{PF}}$. Continuing this off-axis fixed point, we find a Hopf bifurcation at $\varepsilon_{\mathrm{Hopf}}$; see Fig. 2(b). We may then continue along the resulting branch of limit cycles, finding that their periods increase considerably, whihc ε rapidly settles down at a value for which the longest period orbits occur. (At some point, the accuracy of the limit cycle continuation is lost; but by then, ε has settled down sufficiently.) The position of the cycle of longest period is taken as a good approximation to that of the heteroclinic cycle, $\varepsilon_{\mathrm{Het}}$. We observe (see results presented later) that $\varepsilon_{\mathrm{Het}} < \varepsilon_{\mathrm{Hopf}}$; thus the Hopf bifurcation is sub-critical and the limit cycles created are unstable, as predicted by the stability condition (48).

For computations on the systems of dimension three or large, the first bifurcation from the fixed point is a Hopf bifurcation at $\tilde{\varepsilon}_{\mathrm{Hopf}}$, leading to a limit cycle. We continue this limit cycle, monitoring the Floquet multipliers, until it becomes unstable through a torus bifurcation at $\tilde{\varepsilon}_{\mathrm{TR}}$. Since we cannot continue the torus, no further information on stability or the position of a homoclinic/heteroclinic bifurcation can be obtained from AUTO. The relationship between the normal form and the full system implies that we expect $\varepsilon_{\mathrm{PF}} \approx \tilde{\varepsilon}_{\mathrm{Hopf}}$ and $\varepsilon_{\mathrm{Hopf}} \approx \tilde{\varepsilon}_{\mathrm{TR}}$.

5.4.2. Restrictions on ε–δ parameter range

Our restriction to values of δ between 0.0001 and 0.004 was motivated as follows. The lower bound was chosen by considering the scaling for solutions, frequencies for the secondary Hopf bifurcation and separation between bifurcation curves: From the theory for the quadratic normal form of the transcritical/Hopf bifurcation, Section 3, one deduces readily that bifurcating solutions lie at $O(\delta)$ from the origin in phase space, the period of the (secondary) periodic orbit is $O(1/\delta)$, and the separation between the pitchfork and Hopf bifurcation curves is $O(\delta)$. Higher-order analysis (see (46) and (47)) indicates a narrow $O(\delta^2)$ separation between the Hopf and heteroclinic bifurcation curves. This narrow separation, integrator accuracy when computing small solutions, and the difficulty of distinguishing a two-frequency motion with periods of $O(1)$ and $O(1/\delta)$ limits how small we can practically choose δ, and effectively restricts us to $\delta \geq 10^{-4}$. (We use the presence of the transcritical/Hopf bifurcation to determine the presence of a torus and possible chaos, but we need to go some finite distance away in order to have a chance of finding it.) On the other hand, whereas larger parameter values lead to more readily detectable solutions, the approximations and transformations we have made are all valid in the limit for small parameters ε and δ, and small solution amplitudes; the normal forms and their bifurcation curves become less accurate for larger δ, as our computations confirm.

There is another restriction to the maximum δ: For unfoldings of the quadratic normal form (15) and (16), it may be shown (Guckenheimer and Holmes, 1986) that the "interesting" behavior, including the secondary Hopf bifurcation and chaos, occurs only for $a > 0$. Since we do not have a general unfolding for the normal forms (29)–(31), we cannot make a clear statement in this case; but it seems plausible that we need $(a + \kappa\varepsilon + \lambda\delta) > 0$ to find the secondary Hopf bifurcation and torus. For our parameter values for normal forms types I and III, this gives a linear condition for $\delta(\varepsilon)$; at $\varepsilon = 0, \delta < 6.09 \times 10^{-3}$. For the normal form type II (in which λ changes), the δ range becomes even smaller: $\delta < 4.51 \times 10^{-3}$. Indeed, if one uses the continuation facility of AUTO94 to continue the Hopf bifurcation curves in the normal form, one finds that the continuation slows down

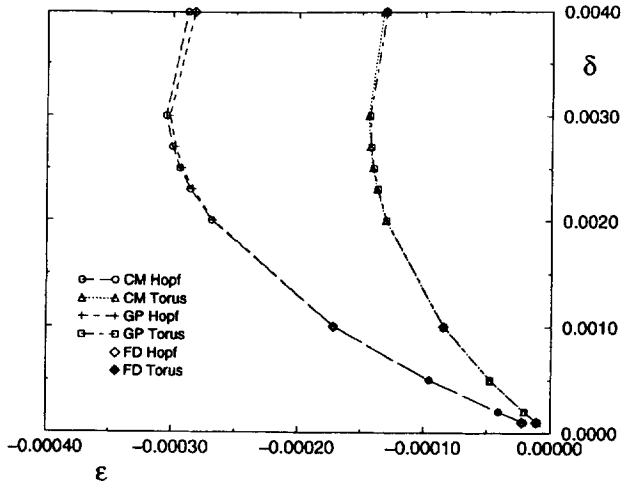

Fig. 5. Primary and secondary Hopf bifurcation curves from Galerkin and finite difference solution of PDE, and 3-mode projection onto center manifold.

and ceases for $\delta \approx 0.006$, in accordance with the above predictions. Thus we need to restrict ourselves to small enough δ.

5.4.3. Bifurcation curves for "full" system

We first describe the bifurcation curves obtained for the Galerkin projection (GP), for the finite difference approximation (FD), and the reduction onto the center manifold (CM). The bifurcation sets are given in Fig. 5 (note: only the indicated points were computed; the lines serve to connect points and distinguish the curves). As is evident from the figure, the three-dimensional center manifold reduction gives a good approximation to the bifurcation behavior of the full PDE (as approximated by GP), which improves nearer the origin in ε–δ space. The bifurcation calculation for the fourth-order finite difference solution (FD) was only performed for three values of δ, 0.004, 0.001 and 0.0001, as continuation of the limit cycle for the 78-dimensional system took considerable computer time. The results for FD deteriorate, compared with the other systems, for smaller δ; for $\delta = 0.0001$, the bifurcation values for all other systems, including the normal forms, were much closer to each other than to the finite difference results (although this is not apparent at the scale of Fig. 5). We might expect this: the error in the fourth-order scheme for the spatial derivative in the u equation, for instance, is $\sim h^4 u^{(vi)}(\xi)/90$, where h is the spatial discretization interval; for a dominant $k = 3$ mode, and $h = \pi/40$, this is $\sim 0.0003u$. However, the amplitudes of the limit cycle and torus solutions scale with δ, and are of $O(10^{-3}$–$10^{-4})$ for $\delta = 0.0001$; so the error is of the same order as u^2. Since the error in the discretization of the derivative is comparable to the size of the nonlinear terms in the system of equations (1), we cannot expect such a scheme to be accurate for small ε, δ. This demonstrates the care that is needed with finite difference schemes for such problems, and suggests that Galerkin projection is more reliable for small amplitude solutions.

Thus, in the region between the primary and secondary Hopf bifurcation curves (and indeed beyond that, to $\varepsilon = 0$, where the limit cycle vanishes on colliding with the trivial fixed point, in another Hopf bifurcation), AUTO provides a limit cycle solution for the Galerkin projection equations, which corresponds to a limit cycle solution for the PDE on converting the modal amplitudes back to the original state variables u and v; such a solution is plotted in Fig. 6. Thus we have found a nontrivial, space and time dependent, limit cycle solution for the PDE (1), corresponding essentially to an oscillation between modes 1 and 3, with some small contribution from higher modes. While interesting, this is not quite the spatio-temporal complexity we are looking for.

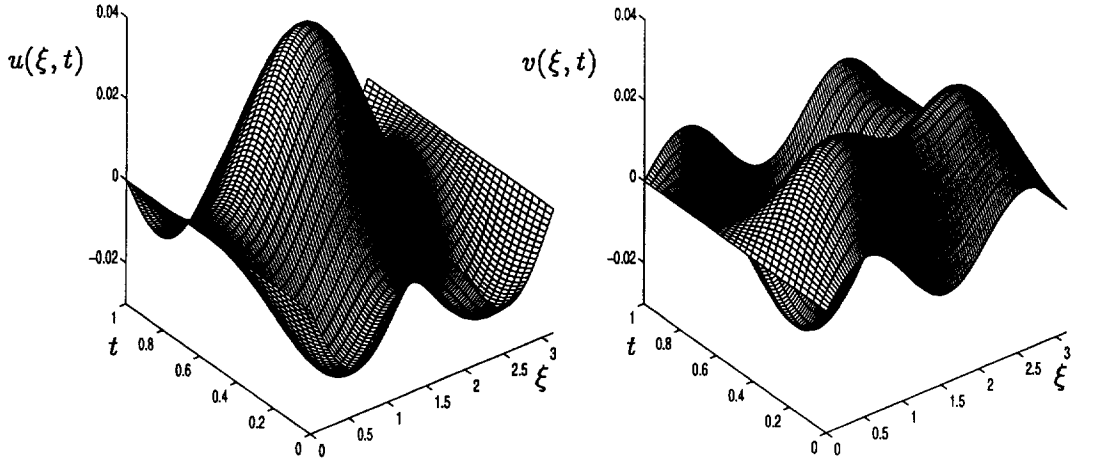

Fig. 6. $u(\xi, t)$ and $v(\xi, t)$ limit cycle solutions for the Brusselator, for parameters $\delta = 0.004$, $\varepsilon = -1.302 \times 10^{-4}$; note the small amplitude of the solutions.

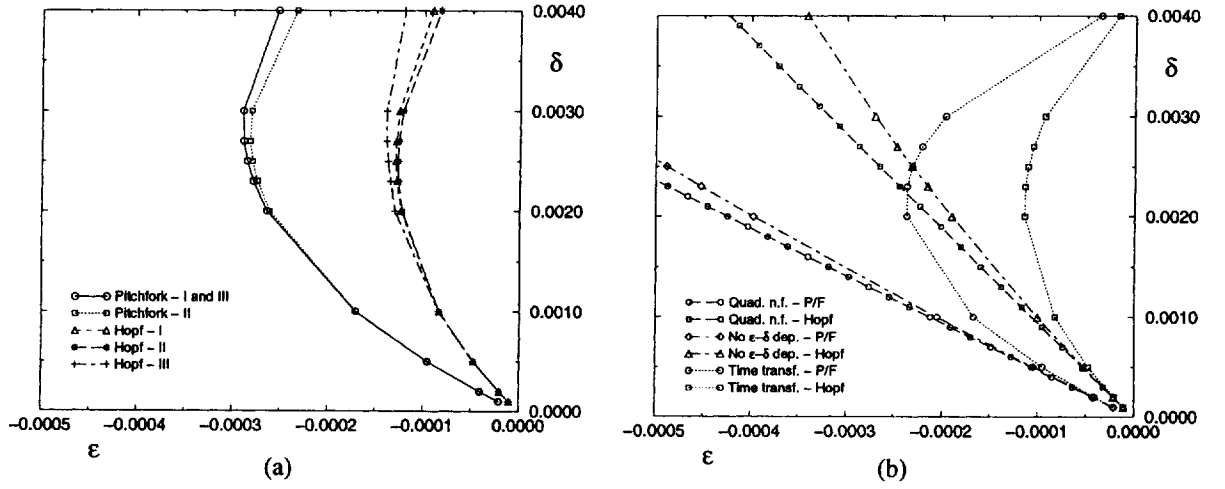

Fig. 7. Pitchfork and Hopf bifurcation curves for (a) the cubic normal forms (41)–(43); and (b) the quadratic normal form, the cubic system (45) without ε–δ dependence, and the cubic system (44) after time transformation. Note of the approximations in (b) compares well with (a).

5.4.4. *Bifurcation curves for normal forms*

We now describe the pitchfork, Hopf and heteroclinic bifurcations for the truncated normal forms and related planar systems (41)–(45). The bifurcation curves are shown in Fig. 7. A comparison between this and Fig. 5 reveals that the cubic normal forms are qualitatively quite good, although they lose quantitative accuracy with increasing δ. The curves for the normal forms, GP and CM are replotted together in Fig. 8, for clear comparison.

It is clear from Fig. 7 that the full cubic normal form is necessary. First of all, the quadratic normal form yields linear bifurcation sets, $\varepsilon_{\mathrm{PF}} = -a\delta$ and $\varepsilon_{\mathrm{Hopf}} = -\frac{1}{2}a\delta$, tangent both to the curves for the cubic normal form and those for the PDE and 3-mode center manifold system at the origin in ε–δ space. (As expected, all bifurcation curves are tangent there; all approximations converge to the "true" solution in the limit as parameters and solution amplitudes tend to zero.) However, at quite modest values – already for $\delta = 0.001$ – these linear approximations are

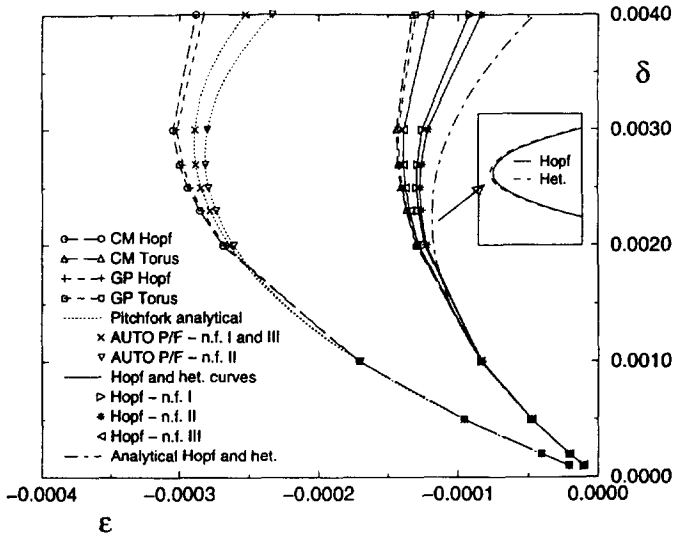

Fig. 8. Hopf and torus bifurcation curves for the full PDE (GP) and the center manifold projection (CM) (compare Fig. 5), and pitchfork and Hopf curves for the cubic normal forms (41)–(43) (compare Fig. 7). Heteroclinic bifurcation curves (solid lines) for the cubic normal forms are also given, as well as analytical approximations (46) and (47) to the Hopf and heteroclinic curves, showing the narrow separation between these curves and the sub-criticality of the Hopf bifurcation.

badly in error. The system (45) lacking the higher-order dependence on ε and δ is similarly inaccurate; it displays the qualitative features of the true curves, but is quantitatively poor, with bifurcation values for $\delta = 0.004$ being in error by about a factor of 2. Hence the point emphasized in Section 4 and Appendix A, that for comparison with the full system, the true dependence on unfolding parameters as in (25) must be respected in the normal form calculations. The system (44), after additional time transformation, fares similarly poorly, although the systematic error is in the opposite direction, relative to the full system. Though the bifurcation curves for the simplified system (32) (still more complicated than (21) and (22), considered in Guckenheimer and Holmes (1986)) are qualitatively indicative, there is too great a cost in accuracy.

We have established that, for any hope of accurate comparison with the full system, the cubic normal form, incorporating the complete ε–δ dependence and without time transformation, is needed. We compare these bifurcation curves for the different types of cubic normal form with those for the "full" system (GP), and with the analytical expressions for the bifurcation curves, in Fig. 8.

5.4.5. *Comparisons*

As indicated previously, the normal form bifurcation curves are remarkably accurate relative to the full bifurcation curves obtained from the 3-mode and 8-mode systems; although not surprisingly, they lose accuracy further from the origin in ε–δ space. Indeed, to the resolution of Fig. 8, all bifurcation points for $\delta \leq 0.001$ are indistinguishable. The pitchfork bifurcation curves for normal forms type I and III are identical, and closer to the "true" curves than that for type II. An exact analytic expression for these curves may be obtained, and confirms the individual bifurcation points numerically computed using AUTO.

For the normal form Hopf bifurcation curves, type III follows the true curves considerably better than types I and II do; this is empirical evidence that of the three possible types of cubic normal form that we have considered, type III (31) is most appropriate for comparison with the full original system. However, studies should be made for other systems than just the Brusselator for our parameter values, in order to confirm this prediction. The $O(\delta^2)$

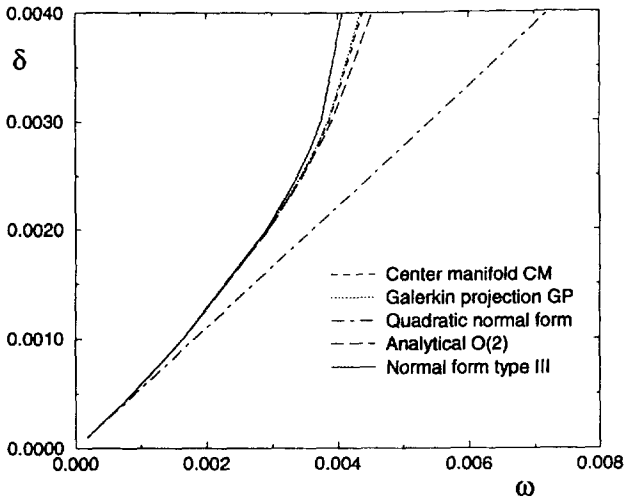

Fig. 9. Frequency of slow motion about torus, for center manifold projection (CM) and full PDE (GP), compared with that predicted from the quadratic normal form, the type III cubic normal form (43) and an $O(\delta^2)$ analysis.

approximation (46) for the Hopf bifurcation curve is quite good, and appears to be, for small ε and δ, a best fit to $O(\delta^2)$ to the true bifurcation curves; but it does lose accuracy above $\delta = 0.0015$. However, the accuracy of the analytical curve means that we would expect at least the qualitative analytic predictions, such as those on the stability of the limit cycle (torus) after the Hopf bifurcation, to be accurate.

5.4.6. *Heteroclinic bifurcation*

The analytically calculated Hopf and heteroclinic bifurcation curves, (46) and (47), although distinct, are indistinguishable in Fig. 8 (the insert in this figure is considerably magnified). The separation between them, as calculated above, is extremely narrow: $\varepsilon \sim O(\delta^2)$, for bifurcation curves which for small δ are $\varepsilon \sim O(\delta)$. Similarly, the lines associated with the normal form Hopf bifurcation points in Fig. 8 in fact connect the computed *heteroclinic* bifurcation points, which are distinct from, but extremely close to, the Hopf bifurcation points. As predicted from Gaspard's results, we find from the AUTO computations in all cases that $\varepsilon_{\text{Het}} < \varepsilon_{\text{Hopf}}$; that is, the Hopf bifurcation is sub-critical and the limit cycles (tori) are unstable.

5.4.7. *Frequencies after Hopf bifurcation*

For further comparison between the normal form and the full system, we examine the frequencies generated in the Hopf bifurcations. The frequency of the limit cycle created in the first Hopf bifurcation for the full system corresponds to the frequency of rotation about the z-axis in the normal form, at the pitchfork bifurcation. The lowest-order approximation to this frequency is ω; we may improve this by evaluating $\dot{\theta}$ from the third normal form equation (and thereby for the first time make use of the θ dynamics in the normal form). Carrying out this comparison, the normal form predictions agree within the accuracy of AUTO computations (five significant figures) to those calculated for the full CM and GP systems over the full δ range we have analyzed.

The frequency created in the secondary Hopf bifurcation is that of slow motion around the torus, which corresponds, after appropriate rescaling, to the frequency of Hopf bifurcation in the normal form. Values for this frequency obtained from the normal form type III (43), analytical approximations and the systems CM and GP are compared in Fig. 9. As expected, the quadratic normal form fares poorly, but the cubic normal form yields fairly good results in comparison to the PDE. An $O(\delta^2)$ perturbation analysis for the type III normal form gives the frequency of slow

motion around the torus as

$$\omega_{\mathrm{TR}} = \frac{2\pi}{\omega}\sqrt{\frac{a}{2}}\delta + \frac{2\pi}{\omega}\delta^2\left\{\frac{1}{\sqrt{2a}}\left(\frac{a}{2}(f-\kappa)+\frac{\lambda}{2}\right) - \frac{1}{\omega}\sqrt{\frac{a}{2}}\left(-\frac{1}{2}\omega_\varepsilon a + \omega_\delta + \frac{1}{2}\tilde{c}_1\right)\right\} + \mathrm{O}(\delta^3), \tag{49}$$

where $\tilde{c}_1 = -c_1/b_2$ is the rescaled coefficient of $z\partial_\theta$, and c_1 is found from (A.8); these computed values also agree well with those of CM and GP. The period of the slow motion thus scales as $1/\delta$, being 3.480×10^4 for $\delta = 0.0001$. We hardly expect to be able to distinguish quasi-periodic behavior with such a large $\mathrm{O}(1/\delta)$ frequency ratio. Additionally, the results of Kirk (1993) on resonance and phase-locking on the torus assume low-order relationships between the frequencies, and thus are inapplicable to our situation.

5.4.8. Implications of normal form for full system

By taking the normal form to cubic order, including the parameter dependence fully to higher order and eschewing the time transformation, and then empirically observing that the type III normal form (31) appears most accurate relative to the full system, we have found a normal form that yields bifurcation curves remarkably close to those obtained for the full PDE and the reduced system on the center manifold. However, the range of ε values, for a given δ, in which the torus exists, is far smaller than the differences between the normal form and "full" bifurcation curves. For the full system, we expect the torus to exist in a range of ε-values, of width $\mathrm{O}(\delta^2)$, just below the true Hopf bifurcation curve. Hence the normal form *cannot* effectively predict quantitative parameter ranges in which the torus will exist. Since we expect Šil'nikov chaos in a C^∞-flat region near the parameter domain of torus existence, failure to predict quantitatively the (open) torus parameter range destroys any possibility of predicting the nearby, even narrower chaotic régime.

Our use of the normal form could be more qualitative: For the normal form, the limit cycle (torus) is predicted to exist for ε just below $\varepsilon_{\mathrm{Hopf}}$. This indicates that we should seek the torus in the full system just below the Hopf bifurcation value, in a parameter domain with a thickness which can be obtained from the normal form, or analytical, results. This approach, however, requires that we always actually find the bifurcation curves for the full system (note that CM is probably not a good enough approximation for GP in this case). Thus we have lost one of the main advantages of the normal form approach: the ability to use parameter values from the *normal form* to predict, quantitatively, behavior in the full system.

A further problem, when we relate our problem back to its original reaction–diffusion formulation, is the observation of solutions, even if we know in which parameter domain to search. As indicated in Section 5.3 from the analytical results of Gaspard, and from the numerical results, the torus is unstable, so we do not expect to detect it in practice in forward integrations of the PDE. The magnitudes of the solutions are also extremely small: For $\delta = 0.004$, the maximum values of u and v for the limit cycle are of the order of 0.025, and the amplitudes scale as δ. (This is readily confirmed for the quadratic normal form, and carries over to the cubic case; the solutions of the full system are related to those of the normal form by a rescaling and an O(1) transformation, both of which are independent of δ.) Such solution amplitudes may seem detectable, but we recall that in the original system (1) u and v represent perturbations from the steady state concentrations $X = A_c = 1.299$ and $Y = B_c/A_c = 2.377$. Hence the "interesting" spatio-temporally complex solutions we seek are perturbations of amplitude at least $\mathrm{O}(10^{-2})$ smaller than the steady solutions; as concentrations, they will not be readily detectable. Lastly, we recall the definitions of the parameters ε and δ (39) and (40) as perturbations of O(1) externally imposed concentrations. Even if it is possible to fix the concentrations A and B to the precision needed to enter the desired ε–δ parameter range, with magnitudes $\sim \mathrm{O}(10^{-2})$ and especially the narrow width $\mathrm{O}(\delta^2)$ of this range, it is hardly likely that this would have much relevance for the overall dynamics of this model chemical reaction system.

6. Conclusions

The application of normal forms and the analysis of transcritical/Hopf bifurcation theory to the Brusselator system yields interesting, rigorous results on the presence of a torus and chaos in this system. However, these spatio-temporally complex behaviors exist in such small parameter régimes, and give rise to such small-amplitude solutions and slow secondary oscillations, that they appear to be extremely difficult to detect, and play a negligible role in the global dynamics of the Brusselator. The origin of robust complex and chaotic behavior such as that observed in the Brusselator by Kuramoto (1978) must be sought elsewhere than in such local, codimension two bifurcation theory. These conclusions about the limited applicability of this codimension two bifurcation theory are directly supported only for the Brusselator system and the specific parameter values investigated, but we believe that they might be more generally applicable. It is interesting to observe that Broer and Vegter (1984) came to a similar conclusion when noting that "the flatness of the described Šil'nikov phenomenon ... makes the phenomenon rather unwieldy for physical applications".

In spite of these rather depressing conclusions on the applicability of center manifold reduction and normal forms in studying certain PDEs, we stress that, applied carefully and in the proper parameter ranges, these techniques yield quantitatively accurate as well as qualitatively useful predictions. Indeed, in preparing this critical survey we have extended, corrected and generalized the available analytical tools, and we have shown that generally available computer algebra software (such as Maple) can be used to perform the required calculations on relatively modest workstations. We merely wish to recommend that the methods be used with caution, and that grand claims on their behalf should not be made.

Acknowledgements

This work was supported by the Department of Energy under DoE DE-FG02-95ER25238 and the National Science Foundation under DMS-9508634.

Appendix A. Normal forms

In Section 3, we motivated the need for the calculation of the cubic coefficients in the normal form; here we outline and carry out this calculation, the results of which were sketched in Section 4.

The basic concepts of normal form theory are outlined in Section 2.2; essentially, one seeks a near-identity change of variables to convert a vector field to as simple a form as possible. In the "classical" theory of normal forms for vector fields – frequently associated with the names Poincaré, Takens and Arnol'd – the structure of the normal form depends only on the *linear* part of the vector field, and may be deduced from it fairly straightforwardly by considering *resonant* terms (Arnol'd, 1988); nonresonant terms may always be removed by a change of variables. The resonant terms may frequently be found purely by symmetry considerations so that, for general classification purposes, no explicit transformations need be carried out. An important feature of the normal form is that it retains the symmetry of the linear part of the vector field. An extensive theory of normal forms has developed, covering a range of different cases – the transformation can, for instance, be chosen to retain global vector field symmetries or Hamiltonian structure; see Bruno (1989) and Chow et al. (1994).

For our purposes of comparison of the normal form with a PDE, it is however necessary to obtain the actual *coefficients* in the normal form. The calculation of these in terms of the original vector field requires us to approximate the actual change of variables.

A.1. Cubic normal form for transcritical/Hopf bifurcation and nonuniqueness

We apply the standard normal form theory to the three-dimensional vector field

$$\dot{x} = -\omega y + f(x, y, z), \qquad \dot{y} = \omega x + g(x, y, z), \qquad \dot{z} = h(x, y, z),$$

where f, g and h are O(2). It is convenient to work in complex coordinates, $\xi = x + \mathrm{i}y$, $\bar{\xi} = x - \mathrm{i}y$, in which the linear part A becomes diagonal,

$$A = \begin{pmatrix} \omega\mathrm{i} & 0 & 0 \\ 0 & -\omega\mathrm{i} & 0 \\ 0 & 0 & 0 \end{pmatrix}.$$

The resonant terms are $\xi(\xi\bar{\xi})^m z^n \partial_\xi$, $\bar{\xi}(\xi\bar{\xi})^m z^n \partial_{\bar{\xi}}$ and $(\xi\bar{\xi})^m z^n \partial_z$ (Chua and Kokubu, 1989). Converting to cylindrical polar coordinates, $r^2 = \xi\bar{\xi}$, $\theta = \arg\xi$, we obtain the normal form

$$\dot{r} = a_1 r z + a_2 r^3 + a_3 r z^2 + \mathrm{O}(4), \tag{A.1}$$

$$\dot{z} = b_1 r^2 + b_2 z^2 + b_3 r^2 z + b_4 z^3 + \mathrm{O}(4), \tag{A.2}$$

$$\dot{\theta} = \omega + c_1 z + c_2 r^2 + c_3 z^2 + \mathrm{O}(3). \tag{A.3}$$

More generally, $\dot{\theta}$, $\dot{z}$ and $r\dot{r}$ are functions only of (r^2, z); this arises through the SO(2) invariance to rotations in the x–y plane in the linear part of the vector field, which implies $r \to -r$ invariance in the normal form, and its independence of θ – the normal form is symmetric to all orders.

In order to obtain the a_j, b_j and c_j in terms of f, g and h, we need to calculate the normal form transformation explicitly to the appropriate finite order. This is best automated using a computer algebra system (Rand and Armbruster, 1987; Chow et al., 1990); the present computations were performed using Maple, on a Silicon Graphics workstation. We postulate a near-identity change of variables,

$$\begin{aligned} \xi &= u + \sum_{\substack{n=2 \\ i+j+k=n}}^{N} a_{ijk} u^i v^j w^k; \qquad \bar{\xi} = v + \sum_{\substack{n=2 \\ i+j+k=n}}^{N} b_{ijk} u^i v^j w^k \quad (b_{ijk} = \bar{a}_{jik}); \\ z &= w + \sum_{\substack{n=2 \\ i+j+k=n}}^{N} c_{ijk} u^i v^j w^k; \end{aligned} \tag{A.4}$$

substitute this into the vector field, and solve for appropriate a_{ijk}, b_{ijk} and c_{ijk} to remove non-resonant terms. After substituting the change of variables, we may remove resonant terms to give the normal form, with coefficients, to order $N + 1$. Specifically, for the cubic normal form, we need only perform the change of variables for $N = 2$.

The results of this calculation yield the normal form coefficients in terms of derivatives of the functions f, g and h. For the quadratic terms in (A.1)–(A.3), we obtain

$$a_1 = \tfrac{1}{2}(f_{xz} + g_{yz}), \tag{A.5}$$

$$b_1 = \tfrac{1}{4}(h_{xx} + h_{yy}), \tag{A.6}$$

$$b_2 = \tfrac{1}{2} h_{zz}, \tag{A.7}$$

$$c_1 = \tfrac{1}{2}(g_{xz} - f_{yz}). \tag{A.8}$$

These quadratic coefficients are unique, and easily found by simply retaining resonant terms from the original vector field (no change of variables is needed).

The cubic terms are found to be:

$$a_2 = \tfrac{1}{16}(f_{xxx} + f_{xyy} + g_{xxy} + g_{yyy}) \qquad (*)$$

$$+ \frac{1}{16\omega}(f_{xy}(f_{xx} + f_{yy}) - g_{xy}(g_{xx} + g_{yy}) - f_{xx}g_{xx} + f_{yy}g_{yy}) \qquad (*)$$

$$+ \frac{1}{32\omega}((f_{yz} + g_{xz})(h_{xx} - h_{yy}) + 2h_{xy}(g_{yz} - f_{xz}))$$

$$+ \tfrac{1}{2}(f_{xz} + g_{yz})c_{110} - \tfrac{1}{4}(h_{xx} + h_{yy})\alpha_{101}, \qquad (A.9)$$

$$a_3 = \tfrac{1}{4}(f_{xzz} + g_{yzz}) + \frac{1}{4\omega}(f_{zz}(f_{xy} + g_{yy}) - g_{zz}(g_{xy} + f_{xx}) + 2(g_{zz}h_{xz} - f_{zz}h_{yz}))$$

$$+ \tfrac{1}{2}(f_{xz} + g_{yz})c_{002} - \tfrac{1}{2}h_{zz}\alpha_{101}, \qquad (A.10)$$

$$b_3 = \tfrac{1}{4}(h_{xxz} + h_{yyz}) + \frac{1}{4\omega}(h_{yz}(f_{xx} + f_{yy}) - h_{xz}(g_{xx} + g_{yy}) + h_{xy}(f_{xz} - g_{yz}))$$

$$+ \frac{1}{8\omega}(f_{yz} + g_{xz})(h_{yy} - h_{xx}) + \tfrac{1}{2}(h_{xx} + h_{yy})(\alpha_{101} - c_{002}) + (h_{zz} - f_{xz} - g_{yz})c_{110}, \qquad (A.11)$$

$$b_4 = \tfrac{1}{6}h_{zzz} + \frac{1}{2\omega}(f_{zz}h_{yz} - g_{zz}h_{xz}), \qquad (A.12)$$

$$c_2 = \tfrac{1}{16}(g_{xxx} + g_{xyy} - f_{xxy} - f_{yyy}) + \frac{1}{48\omega}(f_{xy}g_{xx} + f_{yy}g_{xy} - 2(f_{xx}^2 + f_{xy}^2 + g_{xy}^2 + g_{yy}^2))$$

$$+ \frac{5}{48\omega}(f_{xx}g_{xy} + f_{xy}g_{yy} - f_{yy}(f_{xx} + f_{yy}) - g_{xx}(g_{xx} + g_{yy}))$$

$$+ \frac{1}{32\omega}((g_{yz} - f_{xz})(h_{xx} - h_{yy}) - 2h_{xy}(f_{yz} + g_{xz}))$$

$$+ \tfrac{1}{2}(g_{xz} - f_{yz})c_{110} - \tfrac{1}{4}(h_{xx} + h_{yy})\tilde{\alpha}_{101}, \qquad (A.13)$$

$$c_3 = \tfrac{1}{4}(g_{xzz} - f_{yzz}) - \frac{1}{2\omega}(f_{zz}h_{xz} + g_{zz}h_{yz})$$

$$+ \frac{1}{4\omega}(f_{xz}g_{yz} - f_{yz}g_{xz} - f_{zz}(f_{yy} - g_{xy}) + g_{zz}(f_{xy} - g_{xx}))$$

$$- \frac{1}{8\omega}(f_{xz}^2 + f_{yz}^2 + g_{xz}^2 + g_{yz}^2) + \tfrac{1}{2}(g_{xz} - f_{yz})c_{002} - \tfrac{1}{2}h_{zz}\tilde{\alpha}_{101}, \qquad (A.14)$$

where $a_{101} \equiv \alpha_{101} + \mathrm{i}\tilde{\alpha}_{101}$, and α_{101}, $\tilde{\alpha}_{101}$, c_{110} and c_{002} are free parameters.

Note that at (*) in (A.9) the standard Hopf bifurcation stability formula (Marsden and McCracken, 1976), usually considered to be a complicated calculation in its own right, is here contained as a part of a_2; this provides a useful check on the correctness of our results. Coefficients at orders comparable to the above appear only have been calculated by Spirig (1983), who used an averaging method. Due to the nonuniqueness of the coefficients, discussed below, it is difficult to compare results directly, but the coefficient given above as b_4 is unique, and Spirig's result (given as $\frac{1}{6}\tilde{F}_3^{333}$) is certainly incomplete.

An important feature of the above results is that there are four free coefficients in the transformation, which appear in all cubic terms except b_4. These appear as products with terms which may be recognized as the quadratic normal form coefficients. Hence, assuming that the quadratic terms do not vanish, the cubic normal form is *nonunique*, and we may solve for α_{101}, $\tilde{\alpha}_{101}$, and c_{110} to remove three additional cubic terms (the matrix of coefficients for

α_{101}, $\tilde{\alpha}_{101}$, c_{110} and c_{002} obtained from the above equations is singular, so we cannot solve for all four of these; c_{002} remains undetermined to this order. To remove a fourth cubic term, we need to transform time; see (A.40)). In the case of degeneracy, if the quadratic terms vanish and the first nonzero terms in the normal form are cubic, then the cubic normal form is unique. This occurs for instance if f, g and h are O(3) – in particular, if a symmetry forces the vector field to be odd.

This non-uniqueness has been noted frequently (see Baider and Churchill (1988); Forest and Murray (1994) and Kahn et al. (1995)), but its implications are rarely appreciated. In fact, the most general result on "how well" one can do was presented in 1984 by Ushiki, who used a Lie-algebraic approach and information from nonlinear terms to simplify the normal form beyond that obtained by the Poincaré–Arnol'd–Takens method. An accessible introduction to the Ushiki normal form, using more conventional techniques, was given by Chua and Kokubu (1988, 1989), who also provided worked examples, including the present case. Unfortunately, their approach does not offer a practical way of actually computing the coefficients in the normal form; for that, a change of variables as above must be used, with the Ushiki results merely indicating how well one can do.

Ushiki's theorem for the present case (Ushiki, 1984, Theorem 1.4) is "If the formal vector field in $\mathbb{R}^3$ has a 1-jet at the origin of the form $X^1 = -y\partial_x + x\partial_y$, then X can be "generically" transformed by a formal transformation into a vector field with 5-jet

$$X^5 = \partial_\theta + azr\partial_r + bz\partial_\theta \pm r^2\partial_z \pm z^2\partial_z + cz^3\partial_z + dz^2r\partial_r + ez^2\partial_\theta + fr^5\partial_r + gr^4\partial_\theta, \tag{A.15}$$

where $\partial_\theta = -y\partial_x + x\partial_y$, $r\partial_r = x\partial_x + y\partial_y$, and a, b, c, d, e, f, and g are uniquely determined".

For the reasons noted above, and as we shall see in detail below, the *form* (A.15) is not unique.

A.2. General parameter dependence in the normal form

Before we discuss the different cubic normal forms, there is one other issue to consider. General theory indicates that for a normal form at the bifurcation point such as (A.1)–(A.3), we may obtain a universal unfolding for the transcritical/Hopf bifurcation simply by adding unfolding parameters in the linear terms, as in (19) and (20). However, we are concerned with applications in which the unfolding parameters are given in terms of parameters of the original problem, and wish to relate the parameter range of "interesting" dynamics in the normal form to the original PDE. Apart from some cases in which this was done in an ad hoc way (e.g. Holmes and Rand (1978) and Holmes (1981)), little attention has been paid to this, in spite of its practical importance.

In order to carry out a comparison between the normal form and the PDE, we need an unfolding which respects the parameter dependence of the original system. In the Brusselator system there are two bifurcation parameters, A and B; the parameters ε and δ, defined in (B.9) and (B.10), are perturbations of these parameters from their bifurcation values, or more generally suitable linear combinations thereof, which may be chosen so that the reduced system on the center manifold takes the general form

$$\dot{x} = \varepsilon x - (\omega + \omega_\varepsilon\varepsilon + \omega_\delta\delta)y + f(x, y, z, \varepsilon, \delta), \tag{A.16}$$

$$\dot{y} = (\omega + \omega_\varepsilon\varepsilon + \omega_\delta\delta)x + \varepsilon y + g(x, y, z, \varepsilon, \delta), \tag{A.17}$$

$$\dot{z} = \delta z + h(x, y, z, \varepsilon, \delta). \tag{A.18}$$

From (A.16)–(A.18) we derive the normal form. To do this, we utilize the "suspension trick", adding the equations $\dot{\varepsilon} = 0, \dot{\delta} = 0$, and compute all transformations keeping ε and δ fixed. We remain near the origin in ε–δ space, so all calculations are done to *first order* in ε and δ.

The Poincaré–Takens normal form for this case is again easily deduced from a consideration of resonant terms:

$$\dot{r} = \varepsilon r + a_1 rz + a_2 r^3 + a_3 rz^2 + (\alpha_1\varepsilon + \alpha_2\delta)rz + \mathrm{O}((|\varepsilon| + |\delta|)^2) + \mathrm{O}(4), \tag{A.19}$$

$$\dot{z} = \delta z + b_1 r^2 + b_2 z^2 + b_3 r^2 z + b_4 z^3 + (\beta_1\varepsilon + \beta_2\delta)r^2 + (\beta_3\varepsilon + \beta_4\delta)z^2 + \mathrm{O}((|\varepsilon| + |\delta|)^2) + \mathrm{O}(4), \tag{A.20}$$

$$\dot{\theta} = \omega + \omega_\varepsilon\varepsilon + \omega_\delta\delta + c_1 z + c_2 r^2 + c_3 z^2 + (\gamma_1\varepsilon + \gamma_2\delta)z + \mathrm{O}((|\varepsilon| + |\delta|)^2) + \mathrm{O}(3). \tag{A.21}$$

It turns out, from Ushiki's results and from actual calculation of the transformations, that several of the parameter-dependent third-order terms may be removed, provided the second-order terms are nondegenerate. In particular, we can remove four of the ε–δ coefficients $\alpha_{1,2}$, $\beta_{1,2,3,4}$, $\gamma_{1,2}$. We are less concerned with terms from the $\dot{\theta}$ equation, which uncouples from the other two; so we choose for all future work to remove the coefficients β_1–β_4 in the $\dot{z}$ equation. This leads to the nondegenerate 3-jet of the normal form

$$\dot{r} = \varepsilon r + (a_1 + \alpha_1\varepsilon + \alpha_2\delta)rz + a_2 r^3 + a_3 rz^2, \tag{A.22}$$

$$\dot{z} = \delta z + b_1 r^2 + b_2 z^2 + b_3 r^2 z + b_4 z^3, \tag{A.23}$$

$$\dot{\theta} = \omega + \omega_\varepsilon\varepsilon + \omega_\delta\delta + (c_1 + \gamma_1\varepsilon + \gamma_2\delta)z + c_2 r^2 + c_3 z^2. \tag{A.24}$$

In this normal form, further simplification is possible, due to the nonuniqueness noted earlier. Two of the coefficients a_2, a_3 and b_3 may be chosen to vanish, as may one of c_2 and c_3. This is achieved by solving for the transformation coefficients α_{101}, $\tilde{\alpha}_{101}$, and c_{110} (c_{002} remains undetermined, as discussed above).

As an example of the final results that are obtained, we list the minimal normal form in which the third-order terms a_3, b_3 and c_3 have been eliminated:

$$\dot{r} = \varepsilon r + (a_1 + \alpha_1\varepsilon + \alpha_2\delta)rz + a_2 r^3, \tag{A.25}$$

$$\dot{z} = \delta z + b_1 r^2 + b_2 z^2 + b_4 z^3, \tag{A.26}$$

$$\dot{\theta} = \omega + \omega_\varepsilon\varepsilon + \omega_\delta\delta + (c_1 + \gamma_1\varepsilon + \gamma_2\delta)z + c_2 r^2. \tag{A.27}$$

where a_1, b_1, b_2 and c_1 are as in (A.5)–(A.8), and the coefficients of the nonzero third-order terms are, in terms of the functions f, g and h of (A.16)–(A.18):

$$\begin{aligned}
a_2 = {} & \tfrac{1}{16}(f_{xxx} + f_{xyy} + g_{xxy} + g_{yyy}) + \frac{1}{16\omega}(f_{xy}(f_{xx} + f_{yy}) - g_{xy}(g_{xx} + g_{yy}) - f_{xx}g_{xx} + f_{yy}g_{yy}) \\
& + \frac{1}{32\omega}((f_{yz} + g_{xz})(h_{xx} - h_{yy}) + 2h_{xy}(g_{yz} - f_{xz})) \\
& + \frac{f_{xz} + g_{yz}}{f_{xz} + g_{yz} - h_{zz}}\left(\tfrac{1}{8}(h_{xxz} + h_{yyz}) - \frac{1}{16\omega}(f_{yz} + g_{xz})(h_{xx} - h_{yy})\right. \\
& \left. + \frac{1}{8\omega}(h_{yz}(f_{xx} + f_{yy}) - h_{xz}(g_{xx} + g_{yy}) + h_{xy}(f_{xz} - g_{yz}))\right) \\
& + \frac{h_{xx} + h_{yy}}{f_{xz} + g_{yz} - h_{zz}}\left(\tfrac{1}{8}(f_{xzz} + g_{yzz}) + \frac{1}{4\omega}(g_{zz}h_{xz} - f_{zz}h_{yz})\right. \\
& \left. + \frac{1}{8\omega}(f_{zz}(f_{xy} + g_{yy}) - g_{zz}(f_{xx} + g_{xy}))\right),
\end{aligned} \tag{A.28}$$

$$b_4 = \tfrac{1}{6}h_{zzz} + \frac{1}{2\omega}(f_{zz}h_{yz} - g_{zz}h_{xz}), \tag{A.29}$$

$$c_2 = \ldots \text{(180 terms!)}, \tag{A.30}$$

$$\alpha_1 = \tfrac{1}{2}(f_{xz\varepsilon} + g_{yz\varepsilon}) - \frac{1}{2}\frac{h_{zz\varepsilon}}{h_{zz}}(f_{xz} + g_{yz}), \tag{A.31}$$

$$\alpha_2 = \tfrac{1}{2}(f_{xz\delta} + g_{yz\delta}) - \frac{1}{2}\frac{h_{zz\delta}}{h_{zz}}(f_{xz} + g_{yz}) - \frac{1}{2h_{zz}}(f_{xzz} + g_{yzz})$$
$$+ \frac{1}{2\omega h_{zz}}(g_{zz}(f_{xx} + g_{xy} - 2h_{xz}) - f_{zz}(f_{xy} + g_{yy} - 2h_{yz})), \tag{A.32}$$

$$\gamma_1 = \tfrac{1}{2}(g_{xz\varepsilon} - f_{yz\varepsilon}) + \frac{1}{2}\frac{h_{zz\varepsilon}}{h_{zz}}(f_{yz} - g_{xz}), \tag{A.33}$$

$$\gamma_2 = \tfrac{1}{2}(g_{xz\delta} - f_{yz\delta}) + \frac{1}{2}\frac{h_{zz\delta}}{h_{zz}}(f_{yz} - g_{xz}) + \frac{1}{2h_{zz}}(f_{yzz} - g_{xzz})$$
$$+ \frac{1}{2\omega h_{zz}}(g_{zz}(g_{xx} - f_{xy} + 2h_{yz}) + f_{zz}(f_{yy} - g_{xy} + 2h_{xz}))$$
$$+ \frac{1}{2\omega h_{zz}}(f_{yz}g_{xz} - f_{xz}g_{yz}) + \frac{1}{4\omega h_{zz}}(f_{xz}^2 + f_{yz}^2 + g_{xz}^2 + g_{yz}^2). \tag{A.34}$$

The expression for c_2 not given here, appearing in the $\dot{\theta}$ equation, is not so directly relevant for bifurcation studies, while it is extremely complicated, containing 180 terms. (It was, however, used in calculating the frequency of the limit cycle associated with the primary Hopf bifurcation – pitchfork in the normal form – for comparison with that obtained from AUTO computations on the full system, in Section 5.4) Obsessive readers can obtain it from the authors.

The above expressions apply if we retain the term $a_2 r^3 \partial_r$. One obtains similar expressions for a_3 and b_3 on keeping other terms nonzero, but they may be derived from the above formulae through certain simple relations among the normal form coefficients types I, II and III. These relations are given below for the rescaled coefficients.

The number of independent coefficients in (A.22)–(A.24) may be reduced further by rescaling r and z, as in the passage from (8)–(9) to (15)–(16); this furthermore facilitates comparison between different systems. As before, we rescale by $r \to \sqrt{|b_1 b_2|}r$, $z \to -b_2 z$, to obtain for the $\dot{r}$ and $\dot{z}$ equations the form

$$\dot{r} = \varepsilon r + (a + \kappa\varepsilon + \lambda\delta)rz + gr^3 + hrz^2, \tag{A.35}$$
$$\dot{z} = \delta z + br^2 - z^2 + er^2 z + fz^3, \tag{A.36}$$

where

$$a = -\frac{a_1}{b_2}, \quad b = \operatorname{sign}(-b_1 b_2) = \pm 1, \quad e = \frac{b_3}{|b_1 b_2|}, \quad f = \frac{b_4}{b_2^2},$$
$$g = \frac{a_2}{|b_1 b_2|}, \quad h = \frac{a_3}{b_2^2}, \quad \kappa = -\frac{\alpha_1}{b_2}, \quad \lambda = -\frac{\alpha_2}{b_2}. \tag{A.37}$$

As noted earlier, two of e, g and h may be chosen to vanish, so that we get the three types of normal forms given in the text as types I, II and III. For type I (29), we find the coefficient g from expressions (A.6), (A.7) and (A.28) above. For type III (31), we retain e instead of g, and may calculate e from g by the relation

$$e = 2\frac{a+1}{a}g. \tag{A.38}$$

For the normal form type II (30), we retain h instead of g; in addition the coefficient λ of $(\delta rz)\partial_r$ changes to λ_{II}; these may be found from

$$h = \lambda - \lambda_{\mathrm{II}} = -(a+1)g. \tag{A.39}$$

The three normal forms are thus, essentially, all equivalent.

As Guckenheimer and Holmes (1986) point out, a further simplification is possible on rescaling the vector field, that is, multiplying through by a suitably chosen common factor. This is equivalent to a transformation of the time variable, by

$$\tau = (1 + \nu z)^{-1} t. \tag{A.40}$$

Such a transformation with appropriate choice of ν enables one to remove, at cubic order, a further third-order term, that is, one of e, f, g or h, so that only one is left. For consistency with Guckenheimer and Holmes (1986) and (21) and (22) above, we examine the case in which we retain only the $z^3\partial_z$ term. Of course, as may be readily confirmed, the expressions for the coefficients turn out to be the same whether we perform the time transformation on the normal form type I, II or III. Omitting the decoupled $\dot{\theta}$ equation, the resulting planar system is

$$\frac{\mathrm{d}r}{\mathrm{d}\tau} = \varepsilon r + (a + \tilde{\kappa}\varepsilon + \tilde{\lambda}\delta) r z, \tag{A.41}$$

$$\frac{\mathrm{d}z}{\mathrm{d}\tau} = \partial z - r^2 - z^2 + \tilde{f} z^3. \tag{A.42}$$

Here, the remaining cubic coefficients may be found from those in (A.35) and (A.36) by

$$\tilde{f} = f - \frac{2}{3}\frac{a+1}{a} g, \quad \tilde{\kappa} = \kappa + \frac{2}{3}\frac{a+1}{a} g, \quad \tilde{\lambda} = \lambda + \tfrac{4}{3}(a+1) g, \tag{A.43}$$

while the coefficient ν in the time transformation is

$$\nu = -\frac{2}{3}\frac{a+1}{a} g b_2.$$

Strictly speaking, (A.41) and (A.42) is not a normal form in the usual sense, since it is obtained not merely from a near-identity change of variables in the vector field, but also a (near-identity) rescaling or time transformation. Furthermore, the z-range for which this rescaling is valid is limited, as the latter transformation becomes singular for $z = -1/\nu$.

Appendix B. Brusselator – Galerkin projection and parameters

The Galerkin and center manifold method treats the Brusselator partial differential equations (1) by expanding the solution for $u(\xi, t)$ and $v(\xi, t)$ in Fourier sine bases that match the Dirichlet boundary conditions, and projecting onto the lowest modes. Letting

$$u(\xi, t) = \sum_{l=1}^{\infty} \beta_l(t) \sin l\xi, \qquad v(\xi, t) = \sum_{l=1}^{\infty} \gamma_l(t) \sin l\xi, \tag{B.1}$$

the time evolution of the amplitudes of the Fourier modes is given by

$$\dot{\beta}_l = (-l^2 D_1 + (B - 1))\beta_l + A^2 \gamma_l + h_l, \tag{B.2}$$

$$\dot{\gamma}_l = -B\beta_l - (l^2 D_2 + A^2)\gamma_l - h_l; \tag{B.3}$$

where h_l = {quadratic} + {cubic} terms,

$$\{\text{quadratic}\} = \sum_{m,n} \left(2A\beta_m\gamma_n - \frac{B}{A}\beta_m\beta_n \right) \frac{8lmn}{\pi[(m^2 + n^2 - l^2)^2 - 4m^2n^2]}, \tag{B.4}$$

where the sum is taken over $m, n = 1, \ldots, N$ provided $l + m + n$ is odd; and

$$\{\text{cubic}\} = \tfrac{1}{4} \sum_{m,n} \beta_m \beta_n (\gamma_{l-m+n} - \gamma_{-l+m-n} - \gamma_{l-m-n} + \gamma_{-l+m+n} - \gamma_{-l-m+n} + \gamma_{l+m-n} + \gamma_{-l-m-n} - \gamma_{l+m+n}). \tag{B.5}$$

Note that for l even, every term in both the quadratic and cubic terms of h_l contains even modes, so that the subspace $\{\text{even} = 0\}$ is invariant; this corresponds to the symmetry $\xi \to \pi - \xi$ in the original equations.

From the above modal evolution equations, the linear stability of the lth mode is easily obtained from the Jacobian matrix

$$E_l \equiv \begin{pmatrix} B - 1 - l^2 D_1 & A^2 \\ -B & -A^2 - l^2 D_2 \end{pmatrix},$$

as indicated in the text. In particular, mode l is stable if

$$\begin{aligned} \operatorname{trace}(E_l) &= B - 1 - A^2 - l^2(D_1 + D_2) < 0 \\ \det(E_l) &= A^2 + l^2(A^2 D_1 + D_2 - B D_2) + l^4 D_1 D_2 > 0. \end{aligned}$$

Bifurcation occurs whenever there is equality in the above expressions. Following Guckenheimer (1981), we note that there is a pair of pure imaginary eigenvalues in mode 1, and a single zero eigenvalue in mode $k > 1$, if

$$B = B_c \equiv 1 + A_c^2 + D_1 + D_2, \quad A^2 = A_c^2 \equiv D_2 k^2 \frac{D_1 + D_2 - D_1 k^2}{1 + k^2(D_1 - D_2)}. \tag{B.6}$$

For a given k, there are further conditions on D_1 and D_2 that must be satisfied for this bifurcation to occur. The condition that $A^2 > 0$ gives

$$D_1 > \frac{1}{k^2(k^2-2)}, \qquad D_2 > \frac{k^2 - 1}{k^2(k^2-2)}, \qquad D_2 > D_1 + \frac{1}{k^2}, \tag{B.7}$$

while

$$\begin{aligned} \det(E_{k\pm1}) > 0 \quad \Rightarrow \quad & (\pm 2k^5 + 5k^4 \pm 4k^3 + k^2) D_1 (D_1 - D_2) \\ & + (\pm 4k^3 + 6k^2 \pm 2k) D_1 + (\mp 2k - 1) D_2 < 0, \end{aligned} \tag{B.8}$$

which gives for $k = 3$,

$$D_2 > D_1 \left(1 + \frac{161}{7 + 1008 D_1}\right), \qquad D_2 < D_1 \left(1 + \frac{55}{5 + 180 D_1}\right).$$

The permissible parameter domains for $k = 3$ are indicated in Fig. 3; they are further restricted by inequalities on the quadratic coefficients so that the appropriate unfolding is realized.

In the analysis of the bifurcation, the unfolding parameters ε and δ are introduced, corresponding to perturbations of the parameters B and A from their bifurcation values B_c and A_c. The specific forms of these perturbations are chosen so that the normal form equations assume the block-diagonal form

$$\dot{x} = \varepsilon x - \omega(\varepsilon, \delta) y + \text{h.o.t.}, \qquad \dot{y} = \omega(\varepsilon, \delta) x + \varepsilon y + \text{h.o.t.}, \qquad \dot{z} = \delta z + \text{h.o.t.};$$

it turns out to be convenient to use

$$B = B_c + 2\frac{1+k^2D_1}{1+k^2(D_1-D_2)}\varepsilon + \frac{(1-k^2)(D_1+D_2)}{1+k^2(D_1-D_2)}\delta, \tag{B.9}$$

$$A^2 = A_c^2 + 2\frac{k^2D_2}{1+k^2(D_1-D_2)}\varepsilon + \frac{(1-k^2)(D_1+D_2)}{1+k^2(D_1-D_2)}\delta \tag{B.10}$$

The quadratic coefficients in the normal form may be found by applying formulae (A.5)–(A.7) to the vector field obtained after Galerkin projection, linear transformation to diagonalize, and truncation to the three critical modes. These coefficients and their derivation have been reported elsewhere, with some minor errors (Guckenheimer, 1981, 1984; Scheurle and Marsden, 1984). The correct formulae are:

$$a_1 = \frac{2}{\pi A}(k^2BD_2 - A^2(A^2+k^2D_2))\int_0^\pi \sin^2\xi \sin k\xi \, d\xi, \tag{B.11}$$

$$b_1 = \mu\frac{1}{\pi A}\left(B\left(1+\frac{D_2^2}{\omega^2}\right) - 2A^2\left(1+\frac{D_2(1+D_1)}{\omega^2}\right)\right)\int_0^\pi \sin^2\xi \sin k\xi \, d\xi, \tag{B.12}$$

$$b_2 = \mu\frac{2B}{\pi A}(k^4D_2^2 - A^4)\int_0^\pi \sin^3 k\xi \, d\xi, \tag{B.13}$$

where

$$\omega = (\det(E_1))^{1/2} = ((A^2+D_2)(1+D_1) - BD_2)^{1/2}, \qquad \mu = \frac{k^2D_2}{(A^2+k^2D_2)^2 - A^2B}.$$

As is pointed out in the text, the above integrals all vanish for even k (due to the symmetry $\sin k(\pi-\xi) = -\sin k\xi$). The coupling between mode 1 and an even mode thus leads to the more degenerate situation in which the leading nonlinear terms in the normal form are cubic; a case which we do not consider here. The expressions for the coefficients a and b in the rescaled normal form (15) and (16) are cited in (37) and (38).

It is impractical to give explicit formulae analogous to (B.11)–(B.13) for the cubic coefficients $a_2, \ldots, \gamma_2$, directly in terms of the Brusselator parameters. In practice, one chooses specific numerical values of the parameters and computes the vector field on the center manifold (A.16)–(A.18), via computer algebra. Formulae (A.28)–(A.34) may then be used to obtain the normal form coefficients numerically.

Appendix C. Guckenheimer's parameter values: k=5

In Section 5.1 we quoted the parameter values chosen initially by Guckenheimer (1981) (see also Guckenheimer (1984) and Scheurle and Marsden (1984)) to demonstrate the presence of quasi-periodicity and chaos in the Brusselator, and indicated that these give narrower parameter domains for the bifurcation than the $k = 3$ case suited in the main text. In this appendix we substantiate this by quoting some results analogous to those given in Section 5 for Guckenheimer's $k = 5$ case.

Guckenheimer's suggested parameter values are:

$$k = 5, \quad D_1 = 0.02, \quad D_2 = 0.09, \quad B_c = 2.28, \quad A_c^2 = 1.17, \quad \omega = 1.03923,$$

which satisfy conditions (B.7) and (B.8). The eigenvalues in the lowest odd modes are given in Table 3. The largest eigenvalues in modes 3, 7 and 9 are quite near zero, and fall off much less rapidly than for the $k = 3$ case. Hence

Table 3
Eigenvalues in lowest odd modes, for $k = 5$ (the largest eigenvalues in modes 4 and 6 are -1.0484 and -0.05213, respectively)

Mode	Eigenvalues	
1	1.0392i	−1.0392i
3	−0.44 + 0.54406i	−0.44 − 0.54406i
5	0	−2.64
7	−0.19541	−5.08459
9	−0.68301	−8.11699
11	−1.39001	−11.8100
13	−2.28932	−16.1907
15	−3.36777	−21.2722

Table 4
Effect on the normal form type I coefficients of including successively more modes in the center manifold, for $k = 5$ (coefficients for the other normal form types may be found from (A.38) and (A.39); TS denotes the tangent space truncation)

Modes	f	g	κ	λ
TS	−91.771	−1201.4	0.9700	−54.149
7	−78.644	−1199.1	0.9118	−49.255
11	−49.941	−1198.9	0.9118	−49.064
21	−49.610	−1198.9	0.9118	−49.056

we expect the stable modes to have a relatively large effect on the center manifold dynamics, as is supported by the calculation of the normal form coefficients (for the type I normal form (29)) on including successively more modes; see Table 4. The effect of higher modes on f indicates that even modes 11 and above have an appreciable effect on center manifold dynamics, so that unlike in the $k = 3$ case, many more than eight equations will be needed in a Galerkin truncation to capture the full PDE dynamics in the vicinity of the bifurcation. Note also that mode 6 is only very weakly stable, leading to substantial effects if we consider solutions outside the invariant odd subspace.

The calculation of the normal form proceeds as for the $k = 3$ case; with the perturbations ε and δ from the bifurcation values of A and B defined by

$$B = B_c - 4\varepsilon + 3.52\delta, \quad B_c = 2.28,$$
$$A^2 = A_c^2 - 6\varepsilon + 3.52\delta, \quad A_c^2 = 1.17.$$

After performing the center manifold reduction, and using the formulae in Appendix A to calculate the cubic normal form coefficients, we obtain the three types of normal form, for $k = 5$, $D_1 = 0.02$, $D_2 = 0.09$ (compare (41)–(43)):

Type I (keeping $r^3\partial/\partial r$):

$$\begin{aligned} \dot r &= \varepsilon r + (0.0768254 + 0.911817\varepsilon - 49.056404\,\delta) rz - 1198.873566\, r^3, \\ \dot z &= \delta z - r^2 - z^2 - 49.609710 z^3. \end{aligned} \tag{C.1}$$

Type II (keeping $rz^2\partial/\partial r$):

$$\begin{aligned} \dot r &= \varepsilon r + (0.0768254 + 0.911817\varepsilon - 1340.033909\,\delta) rz + 1290.977505\, rz^2, \\ \dot z &= \delta z - r^2 - z^2 - 49.609710 z^3. \end{aligned} \tag{C.2}$$

Type III (keeping $r^2z\partial/\partial z$):

$$\begin{aligned} \dot r &= \varepsilon r + (0.0768254 + 0.911817\varepsilon - 49.056404\,\delta) rz, \\ \dot z &= \delta z - r^2 - z^2 - 33608.0917 r^2 z - 49.609710 z^3. \end{aligned} \tag{C.3}$$

The normal form coefficient values above do not bode well for successful bifurcation studies, in view of the magnitudes of the cubic coefficients and the discrepancy of four or five orders of magnitude between $a = 0.0768...$ and some cubic coefficients. It is due to these more ill- behaved coefficients and their effects on bifurcation behavior that we consider Guckenheimer's $k = 5$ parameter values far less suited for detection of complex dynamics than the $k = 3$ case studied in this paper. A systematic study, analogous to that described in Section 5, would conclude that phenomena such as torus creation and chaos, inferred from the quadratic normal form, exist in a domain near the origin in phase and parameter space much smaller even than that obtained for the $k = 3$ case. Furthermore, such a study would encounter additional impediments, including numerical errors arising from the smallness of solutions, and difficulty in simulating the full PDE as many more than eight modes would be needed in a Galerkin projection.

A single bifurcation calculation suffices to illustrate that $k = 5$ yields extremely small solutions and parameter ranges, and is thus less suitable than $k = 3$. We calculate the pitchfork, Hopf and heteroclinic bifurcations for the cubic normal form of type I (C.1). For $\delta = 5 \times 10^{-4}$ no Hopf bifurcation was detected, demonstrating how narrow the relevant parameter régimes are. For $\delta = 10^{-4}$, there is a pitchfork bifurcation at $\varepsilon = -7.15599 \times 10^{-6}$, and a Hopf bifurcation from the fixed point $r = 4.98500 \times 10^{-5}$, $z = 4.68574 \times 10^{-5}$ at $\varepsilon = -3.90730 \times 10^{-7}$, yielding a limit cycle with period $T_{LC} = 3.50181 \times 10^{5}$ (frequency $\omega_{LC} = 1.79427 \times 10^{-4}$). Comparing this frequency ω_{LC} with the frequency of fast oscillations $\omega = 1.03923$, we note that the quasi-periodic motion on the torus will be extremely difficult to detect, due to the high frequency ratio. Lastly, the heteroclinic bifurcation occurs at about $\varepsilon = -4.8527 \times 10^{-7}$, so that the torus is unstable, as in the $k = 3$ case studied above.

Guckenheimer's parameter values thus yield much more restricted bifurcation parameter régimes and smaller solution magnitudes than the $k = 3$ case. For this reason we chosen to focus our attention on the critical mode $k = 3$ in the main text.

References

Armbruster, D., G. Dangelmayr and W. Güttinger, 1985, Imperfection sensitivity of interacting Hopf and steady-state bifurcations and their classification, Physica D 16, 99–123.

Armbruster, D., J. Guckenheimer and P. Holmes, 1989, Kuramoto–Sivashinsky dynamics on the center-unstable manifold, SIAM J. Appl. Math. 49, 676–691.

Arnol'd, V.I., 1988, Geometrical Methods in the Theory of Ordinary Differential Equations, 2nd Ed. (Springer, New York).

Arrowsmith, D.K. and C.P. Place, 1990, An Introduction to Dynamical Systems (Cambridge University Press, Cambridge).

Auchmuty, J.F.G. and G. Nicolis, 1975, Bifurcation analysis of nonlinear reaction–diffusion equations – I. Evolution equations and the steady state solutions, Bull. Math. Biol. 37, 323–365.

Auchmuty, J.F.G. and G. Nicolis, 1976, Bifurcation analysis of nonlinear reaction–diffusion equations – III. Chemical oscillations, Bull. Math. Biol. 38, 325–350.

Baider, A. and R. Churchill, 1988, Uniqueness and non-uniqueness of normal forms for vector fields, Proc. R. Soc. Edinb. A 108, 27–33.

Broer, H.W. and G. Vegter, 1984, Subordinate Šil'nikov bifurcations near some singularities of vector fields having low codimension, Ergodic Theory Dynamical Systems 4, 509–525.

Bruno, A.D., 1989, Local Methods in Nonlinear Differential Equations (Springer, Berlin).

Carr, J., 1981, Applications of Centre Manifold Theory (Springer, New York).

Carr, J., S.-N. Chow and J.K. Hale, 1985, Abelian integrals and bifurcation theory, J. Differential Equations 59, 413–436.

Chow, S.-N., B. Drachman and D. Wang, 1990, Computation of normal forms, J. Comput. Appl. Math. 29, 129–143.

Chow, S.-N., C. Li and D. Wang, 1989, Uniqueness of periodic orbits of some vector fields with codimension two singularities, J. Differential Equations, 77, 231–253.

Chow, S.-N., C. Li and D. Wang, 1994, Normal Forms and Bifurcation of Planar Vector Fields (Cambridge University Press, New York).

Chua, L.O. and H. Kokubu, 1988, Normal forms for nonlinear vector fields – Part I: Theory and algorithm, IEEE Trans. Circuits and Systems 35, 863–880.

Chua, L.O. and H. Kokubu, 1989, Normal forms for nonlinear vector fields – Part II: Applications, IEEE Trans. Circuits and Systems 36, 51–70.

Doedel, E.J. and X.J. Wang, 1994, AUTO94: Software for continuation and bifurcation problems in ordinary differential equations, Applied Mathematics Report, California Institute of Technology.

Elphick, C., E. Tirapegui, M.E. Brachet, P. Coullet and G. Iooss, 1987, A simple global characterization for normal forms of singular vector fields, Physica D 29, 95–127.

Field, R.J., E. Körös and R.M. Noyes, 1972, Oscillations in chemical systems. II. Thorough analysis of temporal oscillation in the bromate–cerium–malonic acid system, J. Amer. Chem. Soc. 94, 8649–8664.

Field, R.J. and R.M. Noyes, 1974, Oscillations in chemical systems. IV. Limit cycle behaviour in a model of a real chemical reaction, J. Chem. 60, 1877–1884.

Forest, E. and D. Murray, 1994, Freedom in minimal normal forms, Physica D 74, 181–196.

Gaspard, P., 1993, Local birth of homoclinic chaos, Physica D 62, 94–122.

Glendinning, P. and C. Sparrow, 1984, Local and global behavior near homoclinic orbits, J. Stat. Phys. 35, 645–696.

Golubitsky, M., I. Stewart and D.G. Schaeffer, 1988, Singularities and Groups in Bifurcation Theory, Vol. II (Springer, New York).

Guckenheimer, J., 1981, On a codimension two bifurcation, in: Dynamical Systems and Turbulence, eds. D.A. Rand and L.S. Young (Springer, New York) pp. 99–142.

Guckenheimer, J., 1984, Multiple bifurcation problems of codimension two, SIAM J. Math. Anal. 15, 1–49.

Guckenheimer, J., 1986, Multiple bifurcation problems for chemical reactors, Physica D 20, 1–20.

Guckenheimer, J. and P. Holmes, 1986, Nonlinear Oscillations, Dynamical Systems and Bifurcations of Vector Fields (Springer, New York).

Harrison, L.G., 1993, Kinetic Theory of Living Pattern (Cambridge University Press, Cambridge).

Holmes, P., 1980, Unfolding a degenerate nonlinear oscillator: A codimension two bifurcation, Ann. New York Acad. Sci. 357, 473–488.

Holmes, P., 1981, Center manifolds, normal forms and bifurcation of vector fields with application to coupling between periodic and steady motions, Physica D 2, 449–481.

Holmes, P. and J.E. Marsden, 1981, A partial differential equation with infinitely many periodic orbits: Chaotic oscillations of a forced beam, Arch. Rational Mech. Anal. 76, 135–166.

Holmes, P. and D.A. Rand, 1978, Bifurcations of the forced van der Pol oscillator, Quart. Appl. Math. 35, 495–509.

Kahn, P.B., D. Murray and Y. Zarmi, 1995, Computational aspects of normal form expansions, in: Accelerator Physics at the Superconducting Super Collider, eds. Y.T. Yan, J.P. Naples and M.J. Syphers, AIP Conference Proceedings 326, American Institute of Physics, New York.

Keener, J.P., 1976, Secondary bifurcation in nonlinear diffusion reaction equations, Stud. Appl. Math. 55, 187–211.

Kirk, V., 1991, Breaking of symmetry in the saddle–node Hopf bifurcation, Phys. Lett. A. 154, 243–248.

Kirk, V., 1993, Merging of resonance tongues, Physica D 66, 267–281.

Kuramoto, Y., 1978, Diffusion induced chaos in reaction systems, Suppl. Progr. Theoret. Phys. 64, 346–367.

Langford, W.F., 1979, Periodic and steady mode interactions lead to tori, SIAM J. Appl. Math. 37, 22–48.

Levin, S.A. and L.A. Segel, 1985, Pattern generation in space and aspect, SIAM Rev. 27, 45–67.

Marsden, J.E. and M. McCracken, 1976, The Hopf Bifurcation and Its Applications (Springer, New York).

Murray, J.D., 1989, Mathematical Biology (Springer, Berlin).

Nicolis, G. and I. Prigogine, 1977, Self-Organization in Nonequilibrium Systems: From Dissipative Structures to Order through Fluctuations (Wiley, New York).

Prigogine, I. and R. Lefever, 1968, Symmetry breaking instabilities in dissipative systems. II, J. Chem. Phys. 48, 1695–1700.

Rand, R.H. and D. Armbruster, 1987, Perturbation Methods, Bifurcation Theory and Computer Algebra (Springer, New York).

Schaeffer, D.G. and M.A. Golubitsky, 1981, Bifurcation analysis near a double eigenvalue of a model chemical reaction, Arch. Rational Mech. Anal. 75, 315–347.

Scheurle, J. and J. Marsden, 1984, Bifurcation to quasi-periodic tori in the interaction of steady state and Hopf bifurcations, SIAM J. Math. Anal. 15, 1055–1074.

Šil'nikov, L.P., 1965, A case of the existence of a denumerable set of periodic motions Soviet Math. Dokl. 6, 163–166.

Šil'nikov, L.P., 1970, A contribution to the problem of the structure of an extended neighborhood of a rough equilibrium state of saddle-focus type, Math. USSR Sb. 10, 91–102.

Spirig, F., 1983, Sequence of bifurcations in a three-dimensional system near a critical point, J. Appl. Math. Phys. (ZAMP) 34, 259–276.

Takens, F., 1974, Singularities of vector fields, Publ. Math. IHES 43, 47–100.

Thom, R., 1975, Structural Stability and Morphogenesis (Benjamin, Reading, MA; Original French edition (1972) Stabilité Structurelle et Morphogénèse).

Turing, A.M., 1952, The chemical basis of morphogenesis, Philos. Trans. Roy. Soc. London Ser. B 237, 37–72.

Ushiki, S., 1984, Normal forms for singularities of vector fields, Japan J. Appl. Math. 1, 1–37.

van Gills, S.A., 1985, A note on "Abelian integrals and bifurcation theory", J. Differential Equations 59, 437–441.

Zholondek, K., 1984, On the versality of a family of symmetric vector fields in the plane, Math. USSR-Sb. 48, 463–492.